Supporting Information

Thermodynamics of Nucleic Acid "Shape Readout" by an Aminosugar

Hongjuan Xi, Erik Davis, Nihar Ranjan, Liang Xue, David Hyde-Volpe, and Dev P. Arya*

Laboratory of Medicinal Chemistry, Department of Chemistry, Clemson University, Clemson, South Carolina, 29634

Contents.

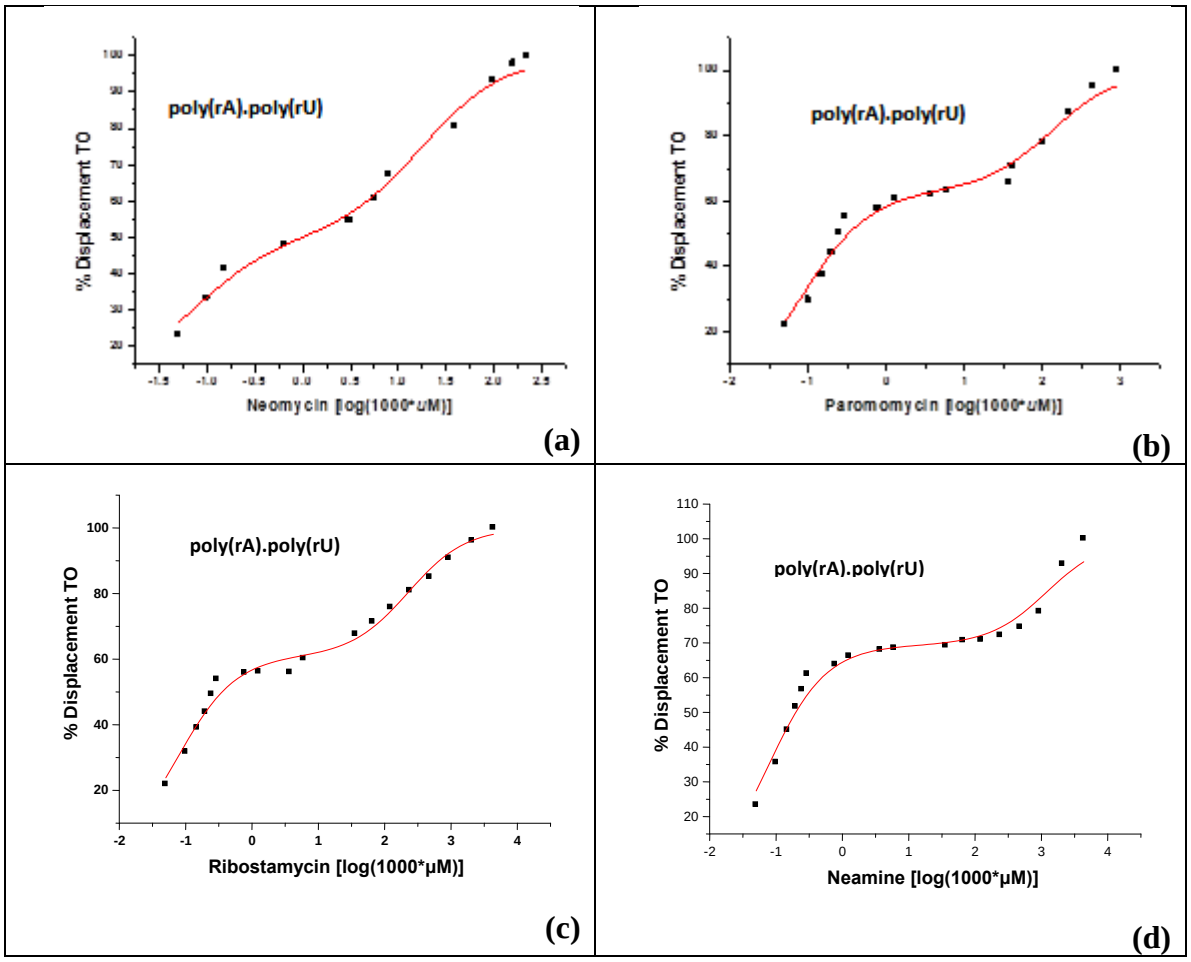

Figure S1. Sigmoidal curve fits for (a) neomycin, (b) paromomycin, (c) ribostamycin, and (d) neamine FID titrations into poly(rA)•poly(rU) duplex using 96 well plate-reader fluorescence. All experiments were carried out in buffer 10 mM sodium cacodylate, 0.5 mM EDTA, 100 mM NaCl at pH 6.8

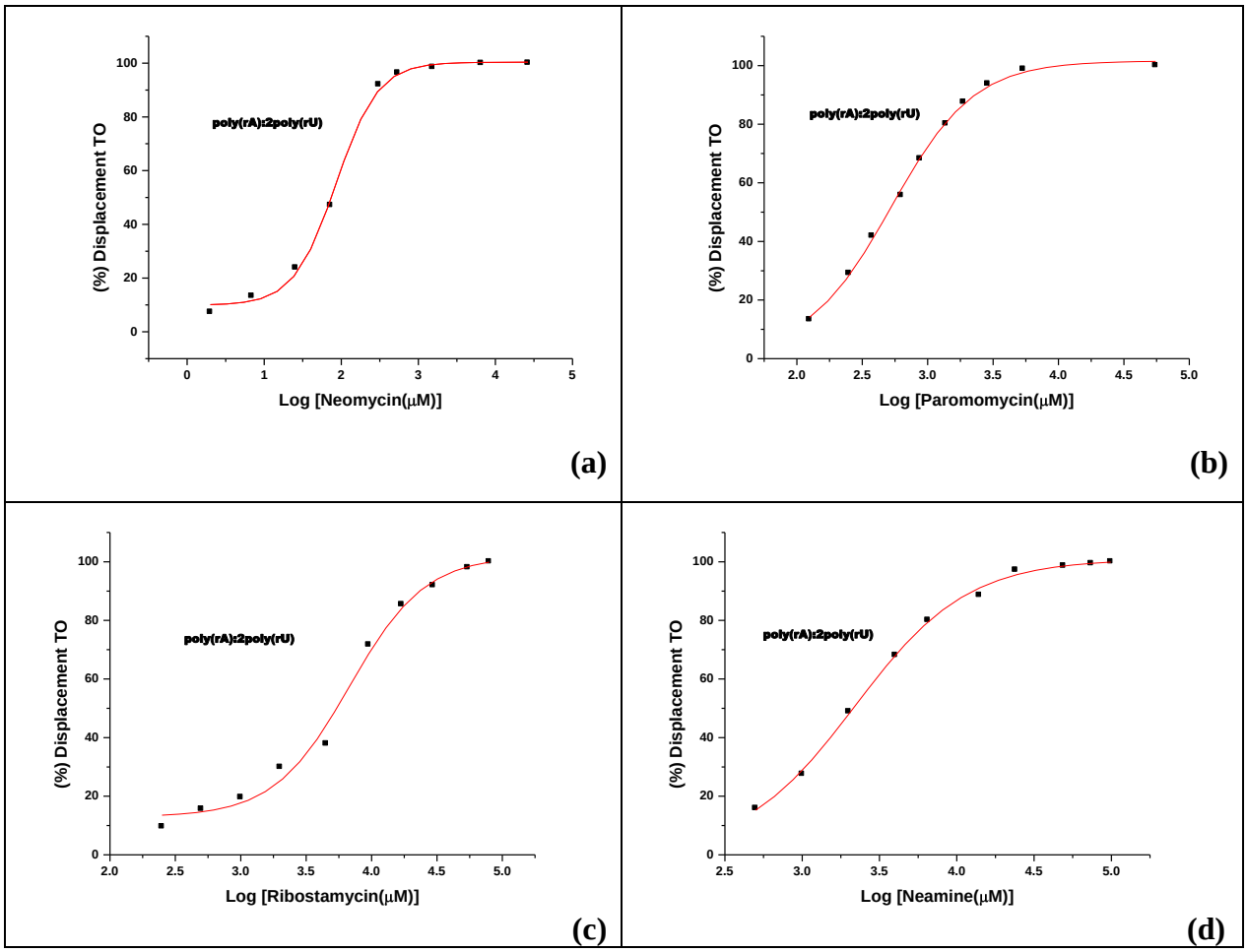

Figure S2. Sigmoidal curve fits for (a) neomycin, (b) paromomycin, (c) ribostamycin, and (d) neamine FID titrations into poly(rA)•2poly(rU) duplex using 96 well plate-reader fluorescence. All experiments were carried out in buffer 10 mM sodium cacodylate, 0.5 mM EDTA, 100 mM NaCl at pH 6.8.

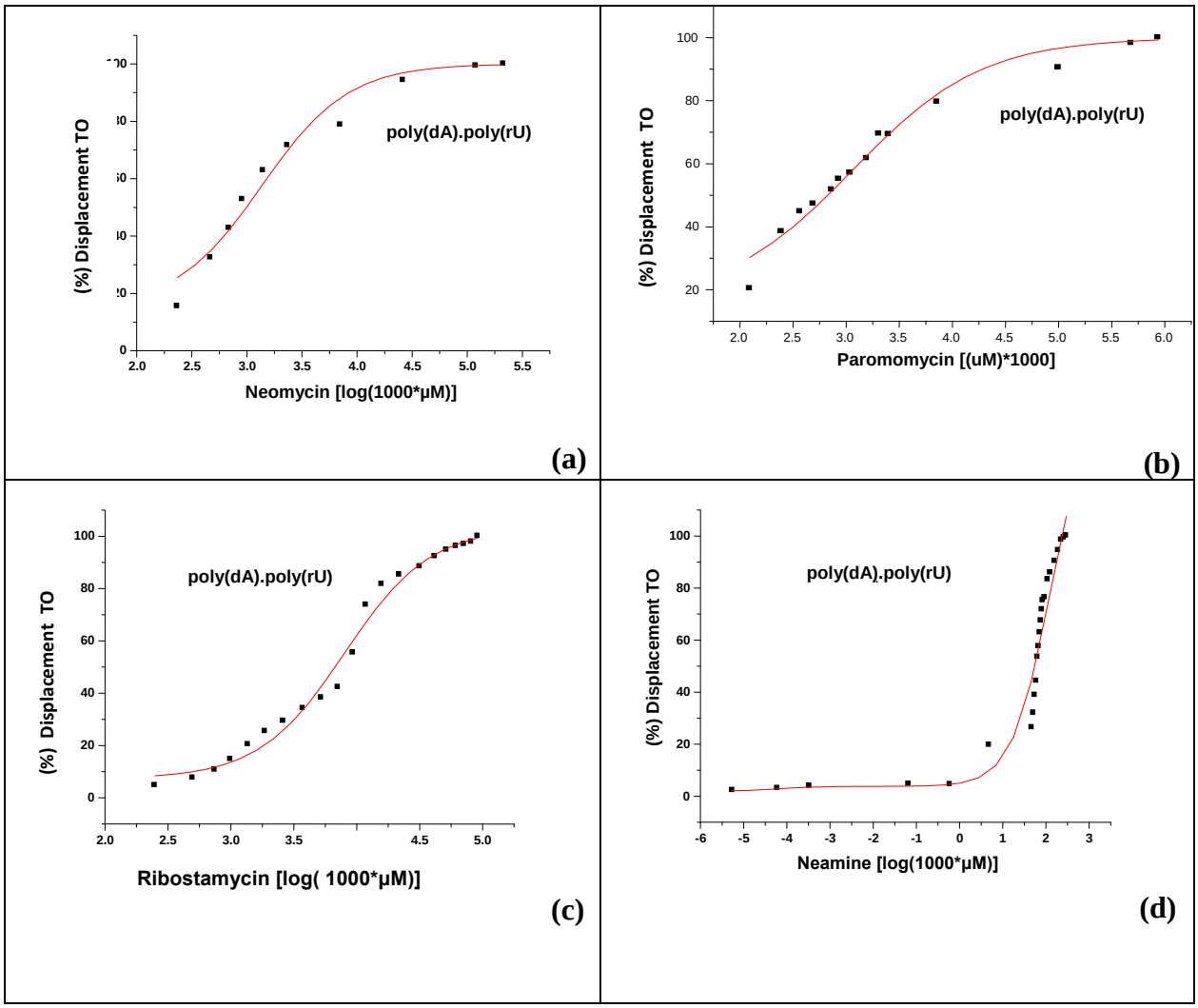

Figure S3. Sigmoidal curve fits for (a) neomycin, (b) paromomycin, (c) ribostamycin, and (d) neamine FID titrations into poly(dA)•poly(rU) duplex using (a-c) 96 well plate-reader fluorescence and (d) fluorescence. All experiments were carried out in buffer 10 mM sodium cacodylate, 0.5 mM EDTA, 100 mM NaCl at pH 6.8.

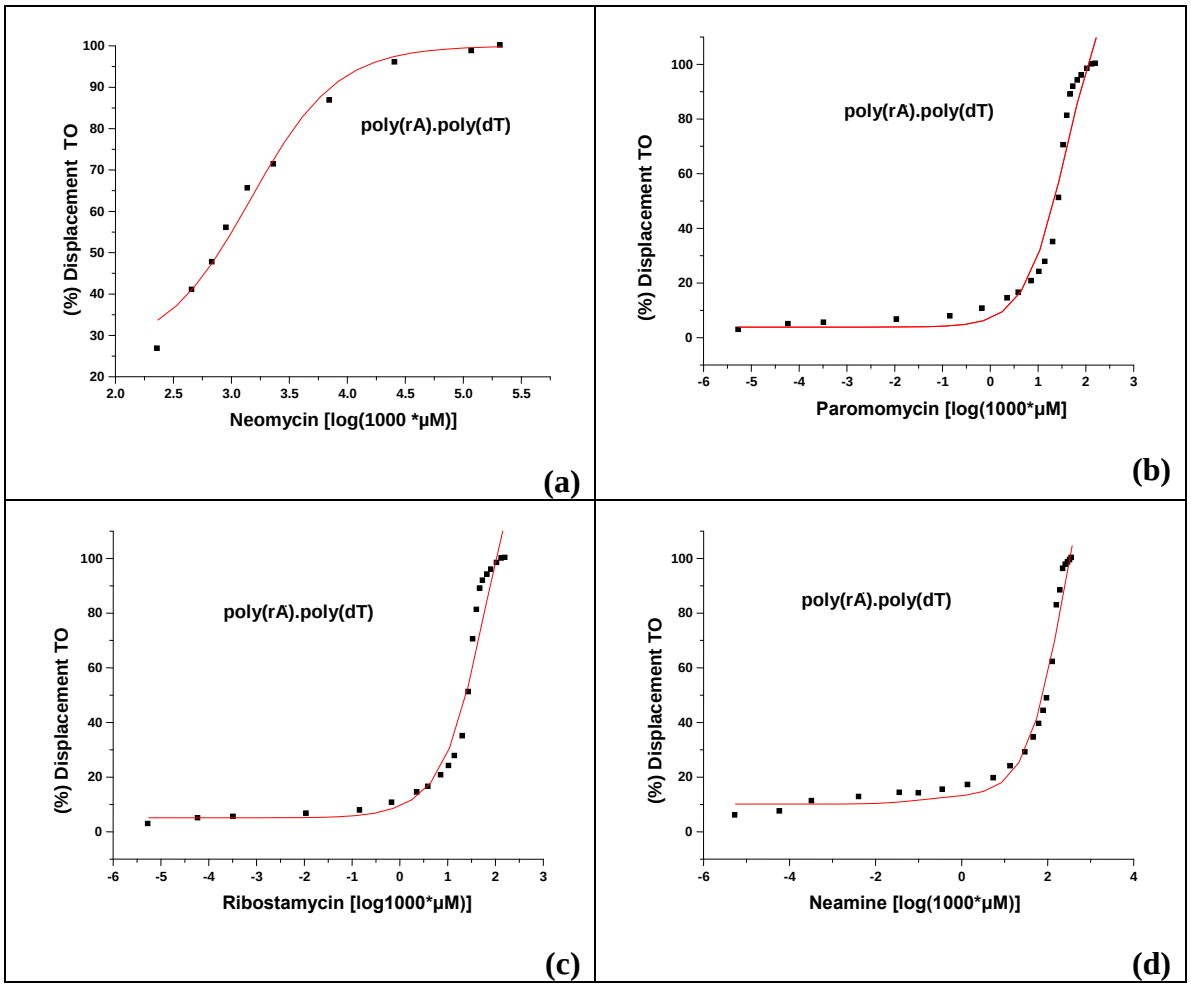

Figure S4. Sigmoidal curve fits for (a) neomycin, (b) paromomycin, (c) ribostamycin, and (d) neamine FID titrations into poly(rA)•poly(dT) duplex using (a) 96 well plate-reader fluorescence and (b-d) fluorescence. All experiments were carried out in buffer 10 mM sodium cacodylate, 0.5 mM EDTA, 100 mM NaCl at pH 6.8.

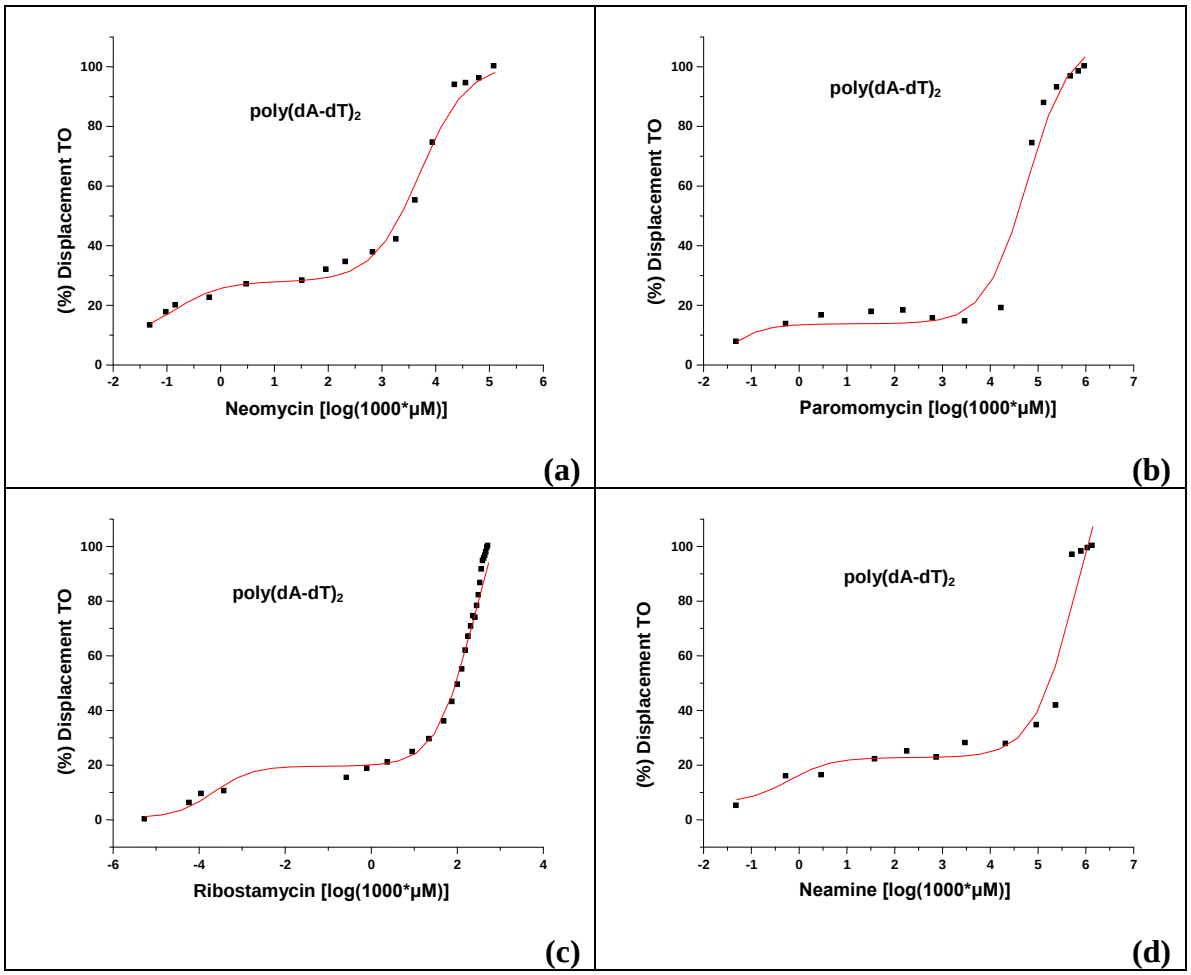

Figure S5. Sigmoidal curve fits for (a) neomycin, (b) paromomycin, (c) ribostamycin, and (d) neamine FID titrations into poly(dT-dT)$_2$ duplex using (a-b, d) 96 well plate-reader fluorescence assays and (c) fluorescence. All experiments were carried out in buffer 10 mM sodium cacodylate, 0.5 mM EDTA, 100 mM NaCl at pH 6.8.

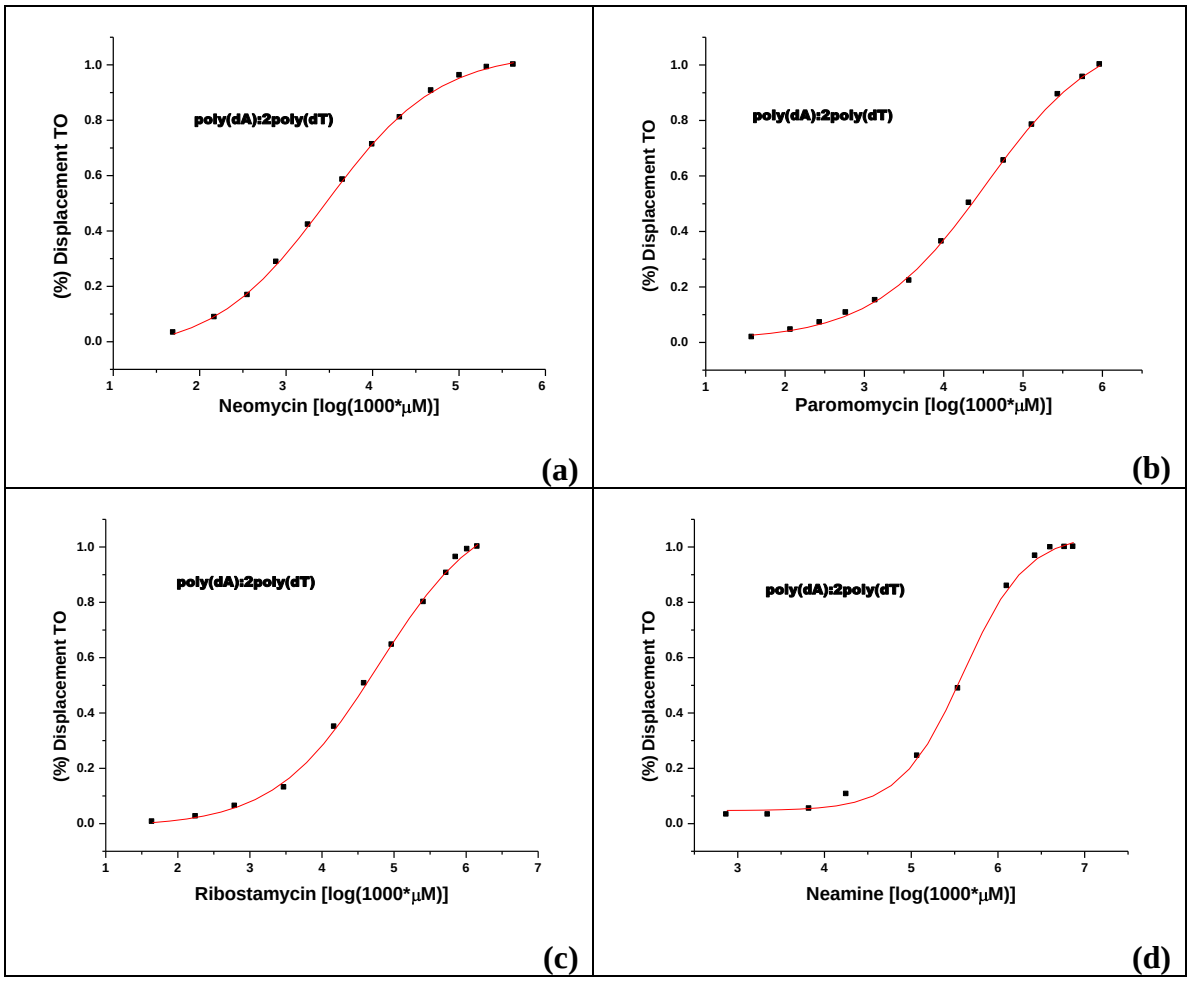

Figure S6. Sigmoidal curve fits for (a) neomycin, (b) paromomycin, (c) ribostamycin, and (d) neamine FID titrations into poly(dA)•2poly(dT) triplex fluorescence titrations. All experiments were carried out in buffer 10 mM sodium cacodylate, 0.5 mM EDTA, 100 mM NaCl at pH 6.8.

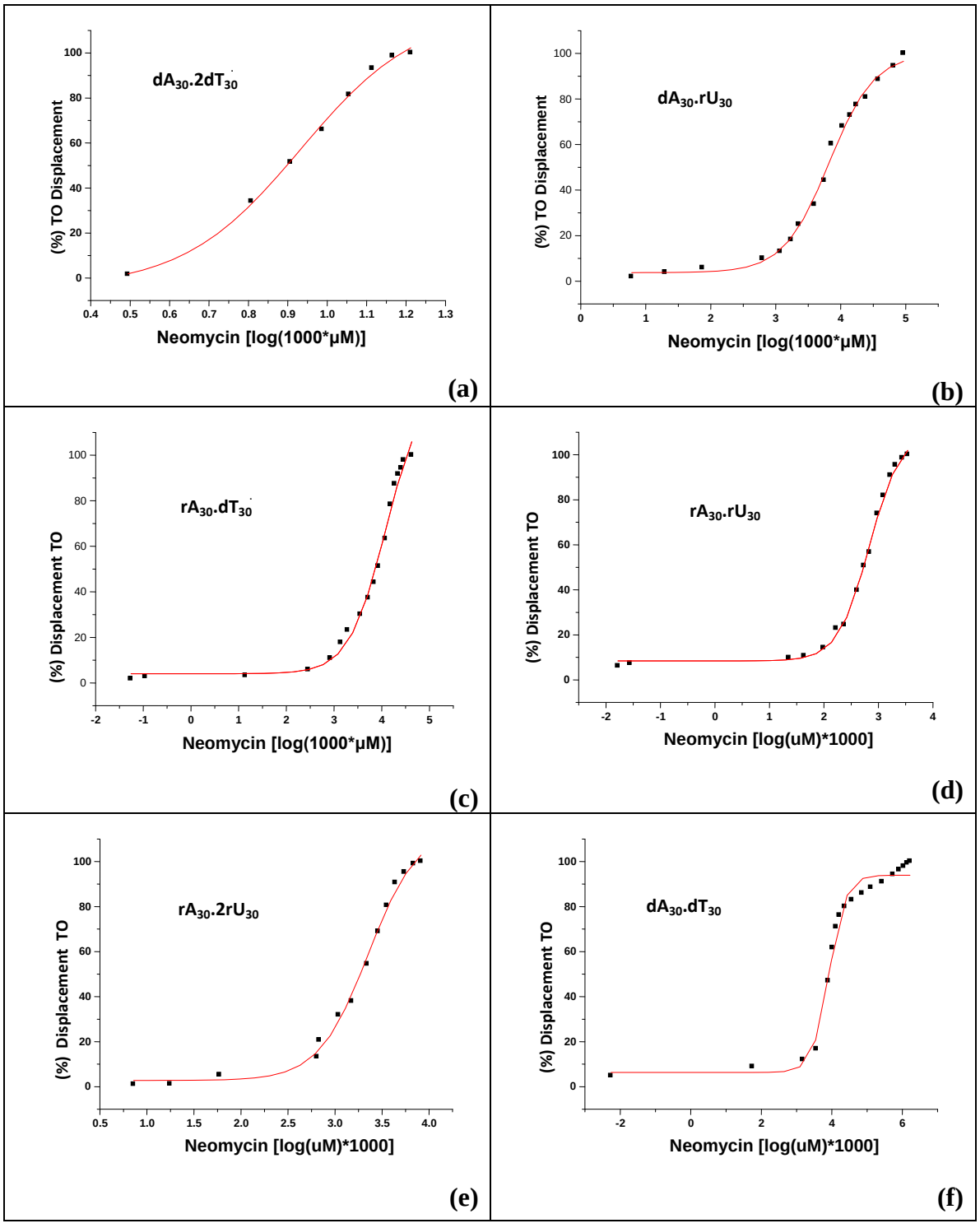

Figure S7. Sigmoidal curve fits for neomycin FID titrations into (a) dA_{30}•$2dT_{30}$, (b) dA_{30}•rU_{30}, (c) rA_{30}•dT_{30}, (d) rA_{30}•rU_{30}, (e) rA_{30}•$2rU_{30}$, (f) dA_{30}•dT_{30} oligomers using fluorescence titrations. Experimental conditions: 1.0 μM nucleotide, 15.0 μM thiazole

orange, 20.0 nM to 5.0 mM aminoglycoside titration. All experiments were carried out in buffer 10 mM sodium cacodylate, 0.5 mM EDTA, 100 mM NaCl at pH 6.8, 10 ^{o}C.

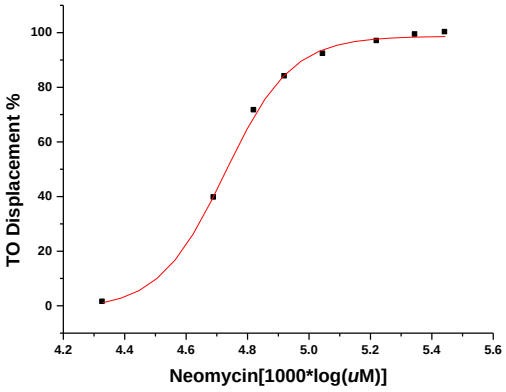

Figure S8. Sigmoidal curve fit for neomycin FID titration into dA_{30}•$2dT_{30}$ using fluorescence titration. Experiment was carried out in buffer 10 mM sodium cacodylate, 0.5 mM EDTA, 100 mM NaCl and 150 mM KCl at pH 6.8, 10 ^{o}C.

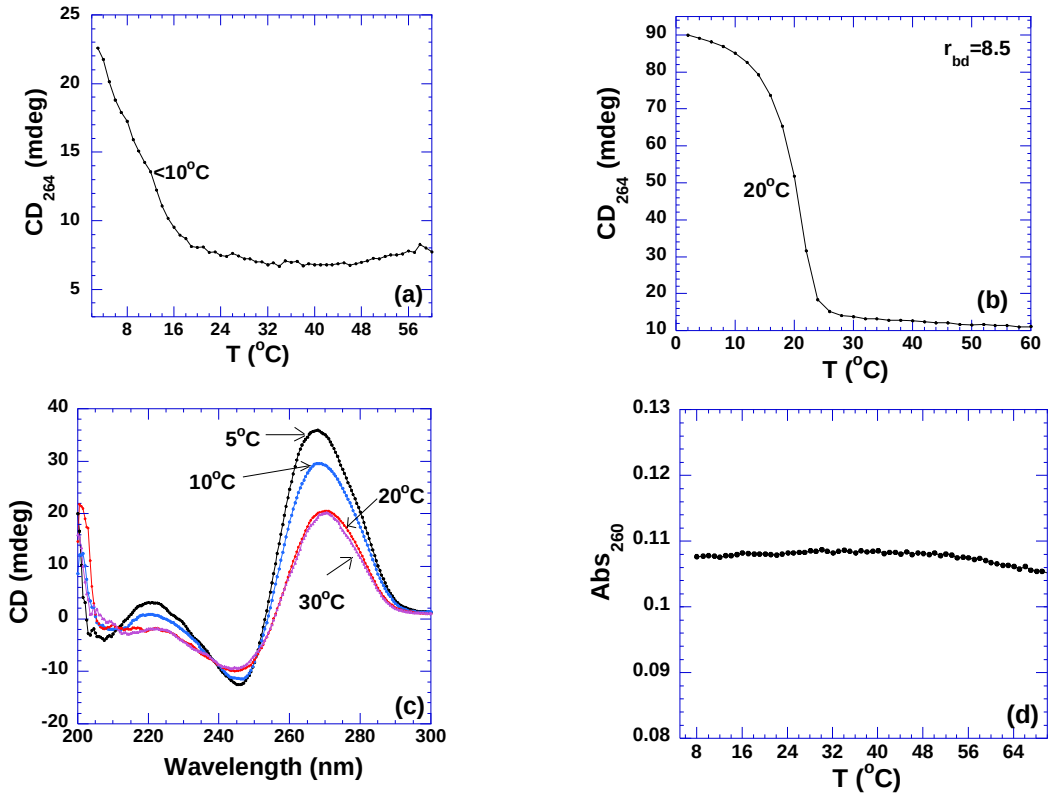

Figure S9. CD melting profiles of poly(rU) (100 μM/strand) in the absence (a) and presence (b) of neomycin at r_{bd} 8.5 at pH 6.8. (c) CD scan of poly(rU) (100 μM/strand) at different temperatures at pH 6.8. (d) UV melting profile of poly(rU) at pH 5.5. Buffer 10 mM sodium cacodylate, 0.5 mM EDTA, 100 mM NaCl.

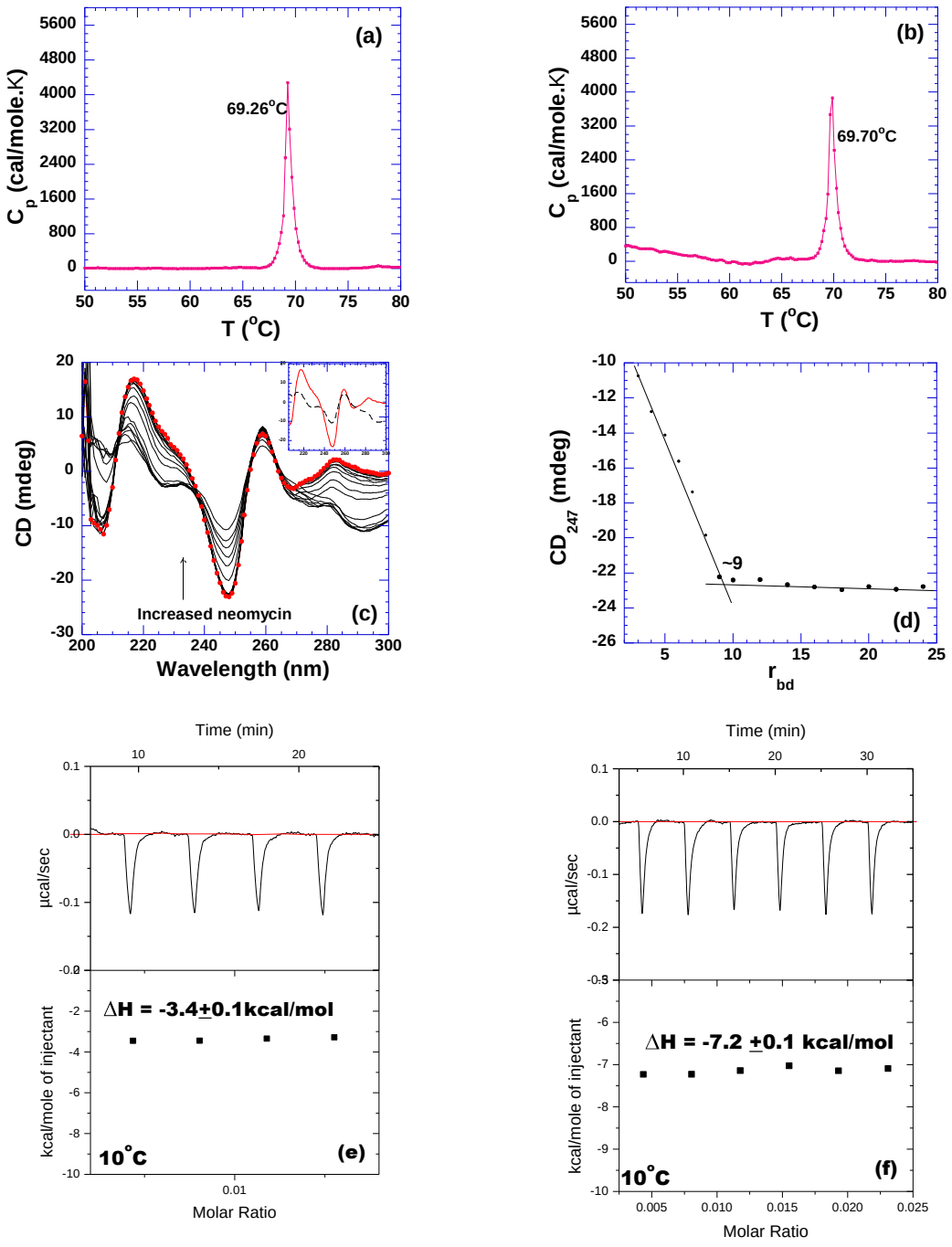

Figure S10. (a,b) DSC melting profiles of poly(dA)•poly(dT) (100 µM/base pair) in the absence (a) and presence (b) of neomycin at r_{bd} 9. (c) CD scans of neomycin titration with poly(dA)•poly(dT) (75 µM/base pair). The scan with solid circle represents DNA alone. The inset shows the CD spectra of DNA alone (continuous line) and ligand-

saturated complex (dashed line). (d) A plot of CD signals at 247 nm *versus* corresponding r_{bd} values. The cross of two apparent linear portions reveals binding site sites. (e) ITC titration of neomycin into poly(dA-dT)$_2$ (150 μM/base pair) at 10 ^{o}C and (f) ITC titration of neomycin into poly(dA)•poly(dT) (150 μM/base pair) 10 ^{o}C. All experiments were carried out in buffer 10 mM sodium cacodylate, 0.5 mM EDTA, 100 mM NaCl at pH 6.8.

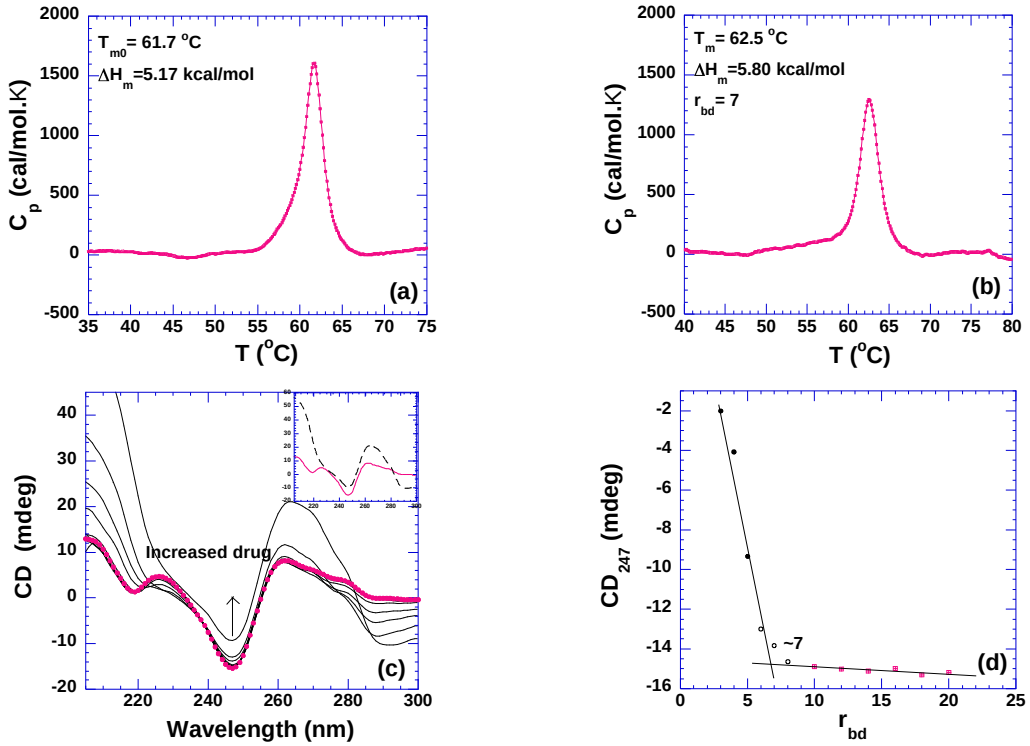

Figure S11. (a,b) DSC melting profiles of poly(dA-dT)$_2$ (100 μM/base pair) in the absence (a) and presence (b) of neomycin. (c) CD scans of neomycin titration with poly(dA-dT)$_2$ (75 μM/base pair). The scan with solid circle represents DNA alone. The inset shows CD spectra of DNA alone (continuous line) and ligand-saturated complex (dashed line). (d) A plot of CD signals at 247 nm *versus* corresponding r_{bd} values. All experiments were carried out in buffer 10 mM sodium cacodylate, 0.5 mM EDTA, 100

mM NaCl at pH 6.8.

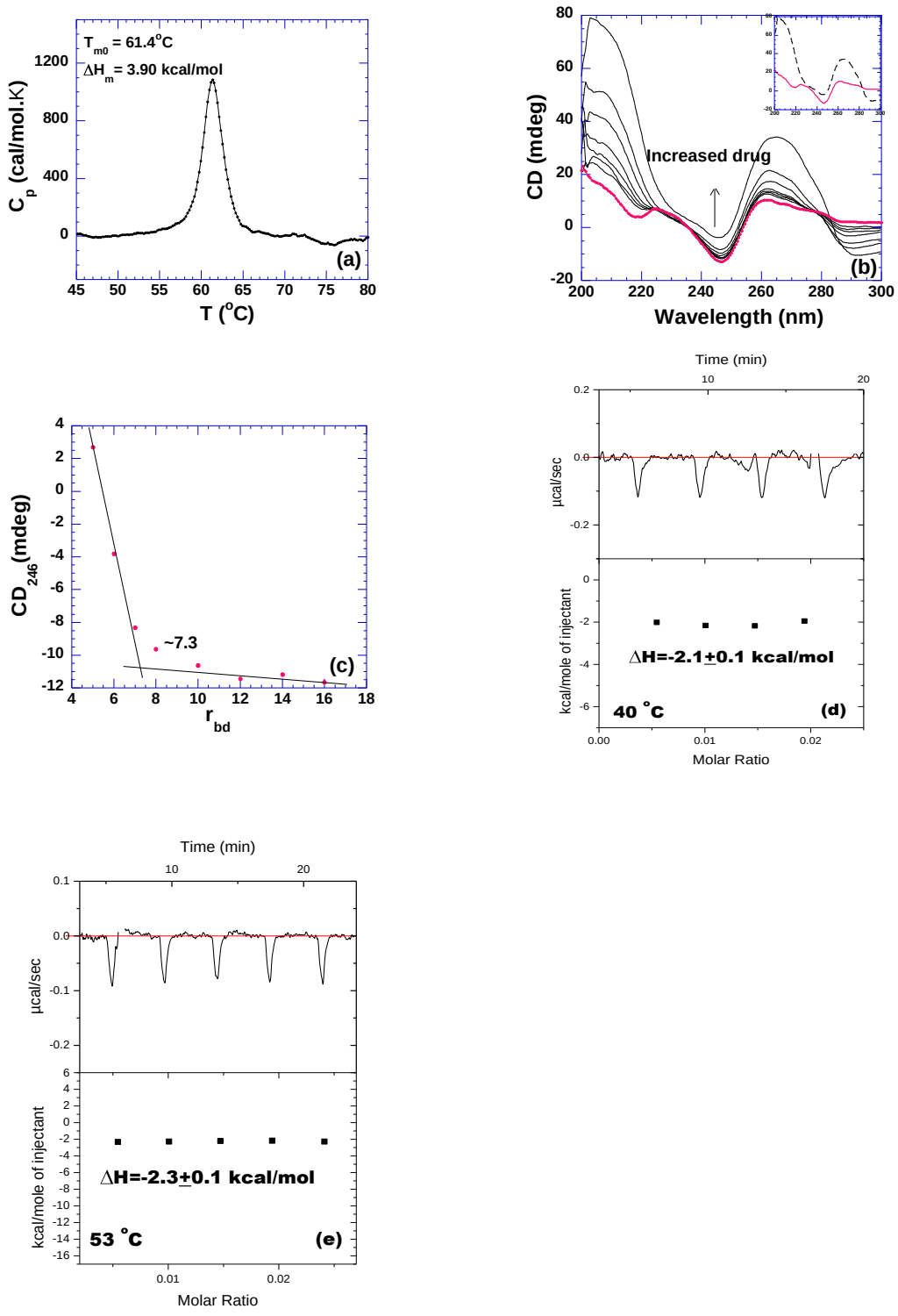

Figure S12. (a) DSC melting profiles of poly(dA-dT)$_2$ (100 µM/base pair) in the absence

of neomycin. (b) CD scans of neomycin titration with poly(dA-dT)$_2$ (75 μM/base pair). The scan with solid circle represents DNA alone. The inset is the CD spectra of DNA alone (continuous line) and ligand-saturated complex (dashed line). (c) A plot of CD signals at 246 nm *versus* corresponding r_{bd} values. (d,e) ITC titration of neomycin into poly(dA-dT)$_2$ (300 μM/base pair) at 40 ^{o}C (e) and 53 ^{o}C (f). All experiments were carried out in buffer 10 mM sodium cacodylate, 0.5 mM EDTA, 100 mM NaCl at pH 5.5.

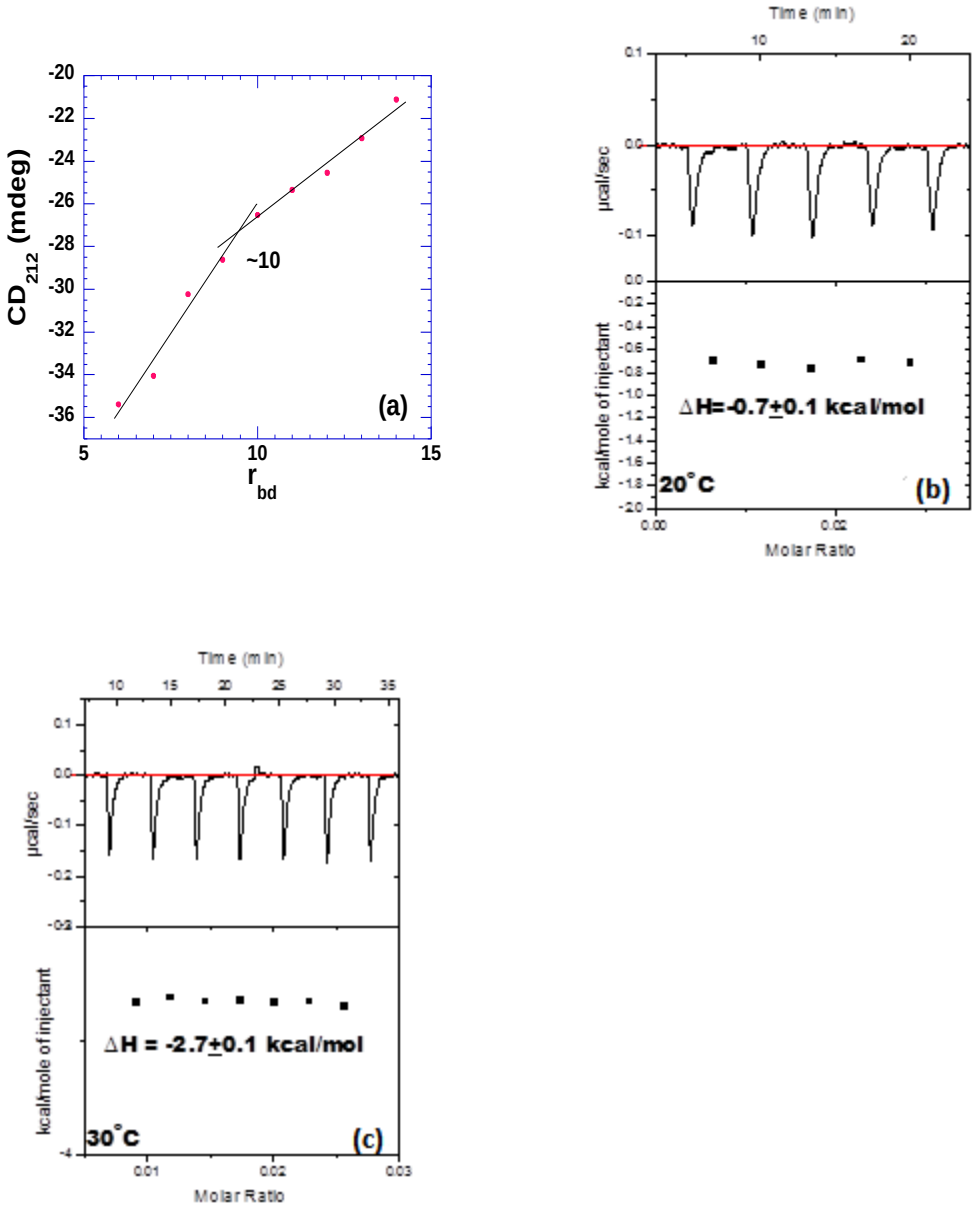

Figure S13. (a) A plot of $d(A_2G_{15}C_{15}T_2)_2$ CD signals at 212nm vs. corresponding r_{bd} values. (b,c) ITC titration of neomycin into $d(A_2G_{15}C_{15}T_2)_2$ (15 µM/duplex) at (b) 20 ^oC and (c) 30 ^oC. All experiments were carried out in buffer 10 mM sodium cacodylate, 0.5 mM EDTA, 100 mM NaCl at pH 5.5.

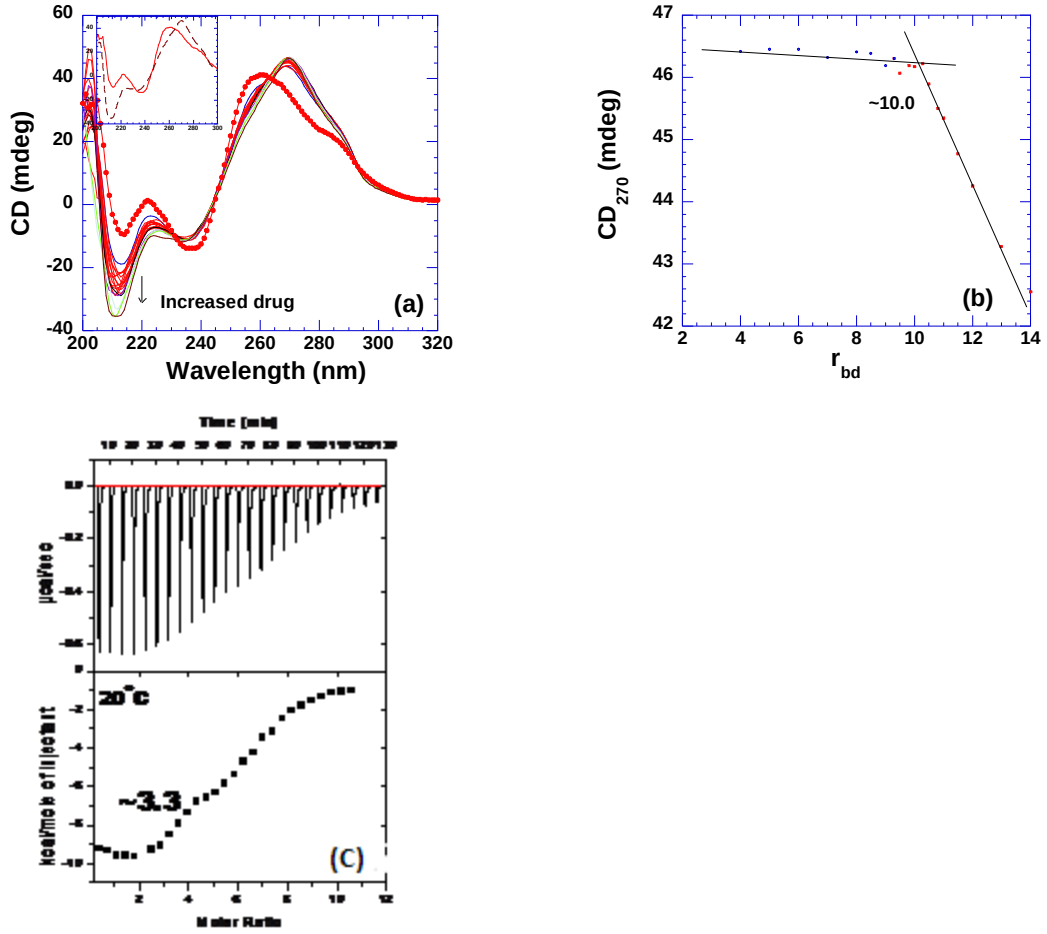

Figure S14. (a) CD scans of neomycin titration with DNA duplex $d(A_2G_{15}C_{15}T_2)_2$ (3 μM/duplex). The scan with solid circle represents DNA alone. The inset shows the CD spectra of DNA alone (continuous line) and ligand-saturated complex (dashed line). (b) A plot of CD signals at 270 nm *versus* corresponding r_{bd} values. The cross of two apparent linear portions reveals binding site sites. (c) ITC titration of neomycin with $d(A_2G_{15}C_{15}T_2)_2$ (40 μM/duplex). The binding site size for first binding event was shown in plot. All experiments were carried out in buffer 10 mM sodium cacodylate, 0.5 mM EDTA, 100 mM NaCl at pH 6.8.

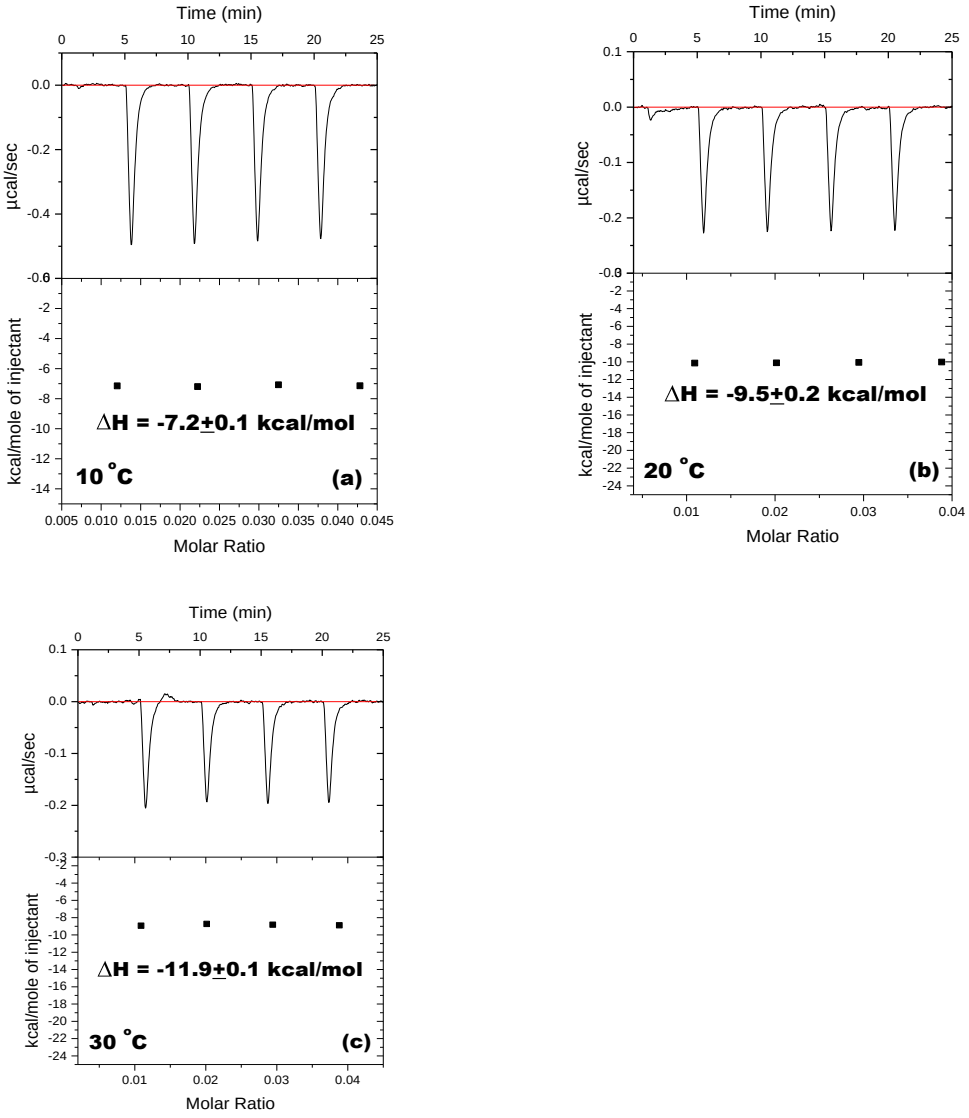

Figure S15. ITC titration of neomycin into $d(A_2G_{15}C_{15}T_2)_2$ (5 µM/duplex) at (a) 10 ^oC, (b) 20 ^oC, and (c) 30 ^oC. All experiments were carried out in buffer 10 mM sodium cacodylate, 0.5 mM EDTA, 100 mM NaCl at pH 6.8.

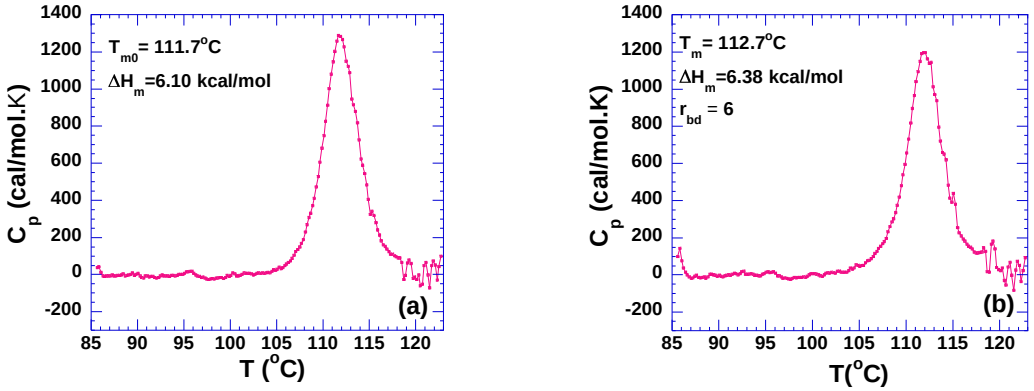

Figure S16. DSC melting profiles of poly(dG-dC)$_2$ (100 μM/base pair) in the absence (a) and presence (b) of neomycin. All experiments were carried out in buffer 10 mM sodium cacodylate, 0.5 mM EDTA, 100 mM NaCl at pH 6.8.

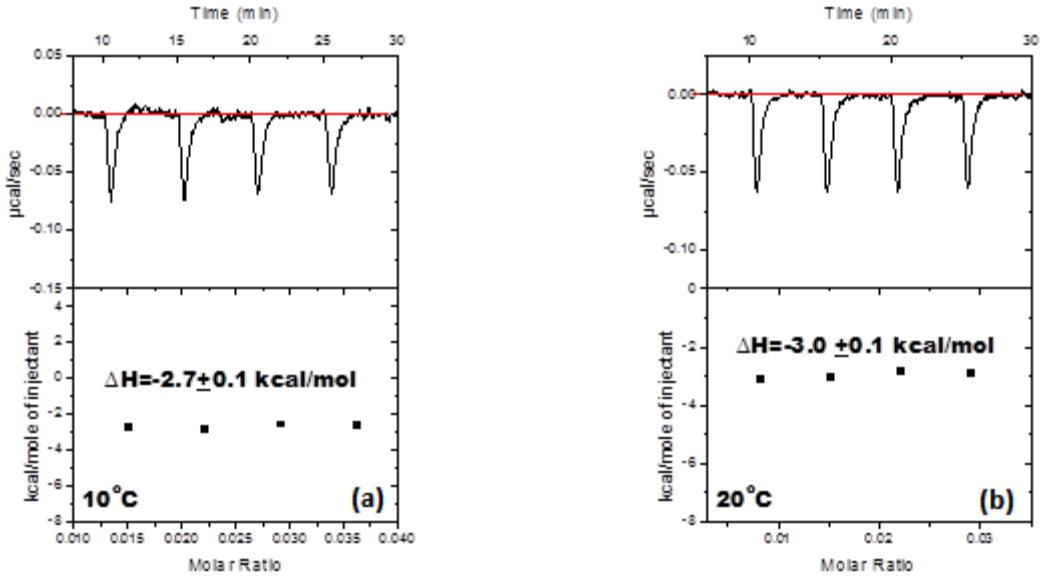

Figure S17. (a) ITC titration of neomycin into poly(dG-dC)$_2$ (75µM/base pair) at 10 ^{o}C and (b) at 20 ^{o}C. All experiments were carried out in buffer 10 mM sodium cacodylate, 0.5 mM EDTA, 100 mM NaCl at pH 6.8.

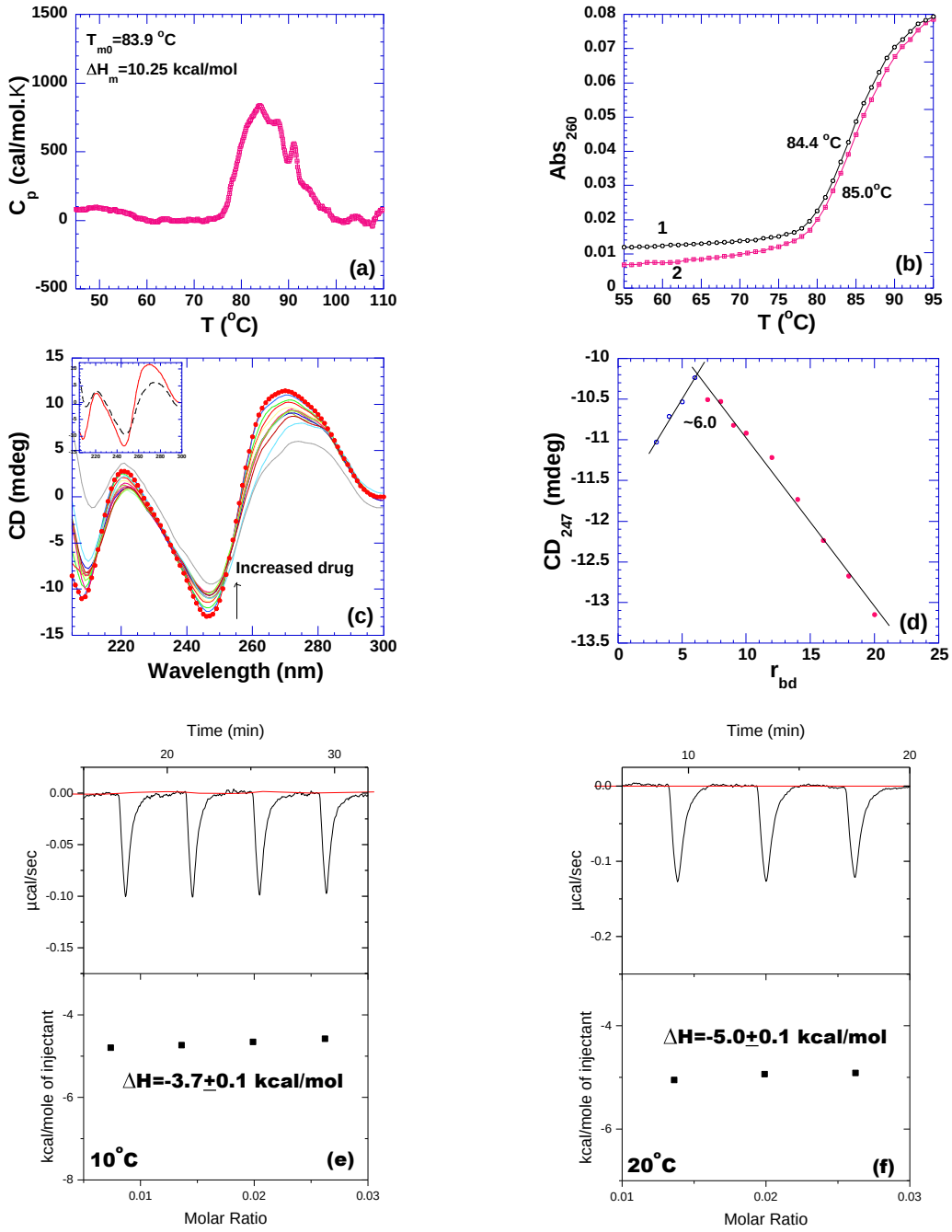

Figure S18. (a) DSC melting profiles of calf thymus (75 µM/base pair) in the absence of neomycin. (b) UV melting profiles of duplex in the absence (1) and presence (2) of neomycin at r_{bd} of 6. (c) CD scans of neomycin titration with calf thymus (40 µM/base pair). The scan with solid circle represents DNA alone. The inset shows the CD spectra

of DNA alone (continuous line) and ligand-saturated complex (dashed line). (d) A plot of CD signals at 247 nm vs. corresponding r_{bd} values. The cross of two apparent linear portions reveals binding site sites. (e,f) ITC titration of neomycin into calf thymus (100 μM/base pair) at 10 ^{o}C (e) and 20 ^{o}C (f). All experiments were carried out in buffer 10 mM sodium cacodylate, 0.5 mM EDTA, 100 mM NaCl at pH 6.8.

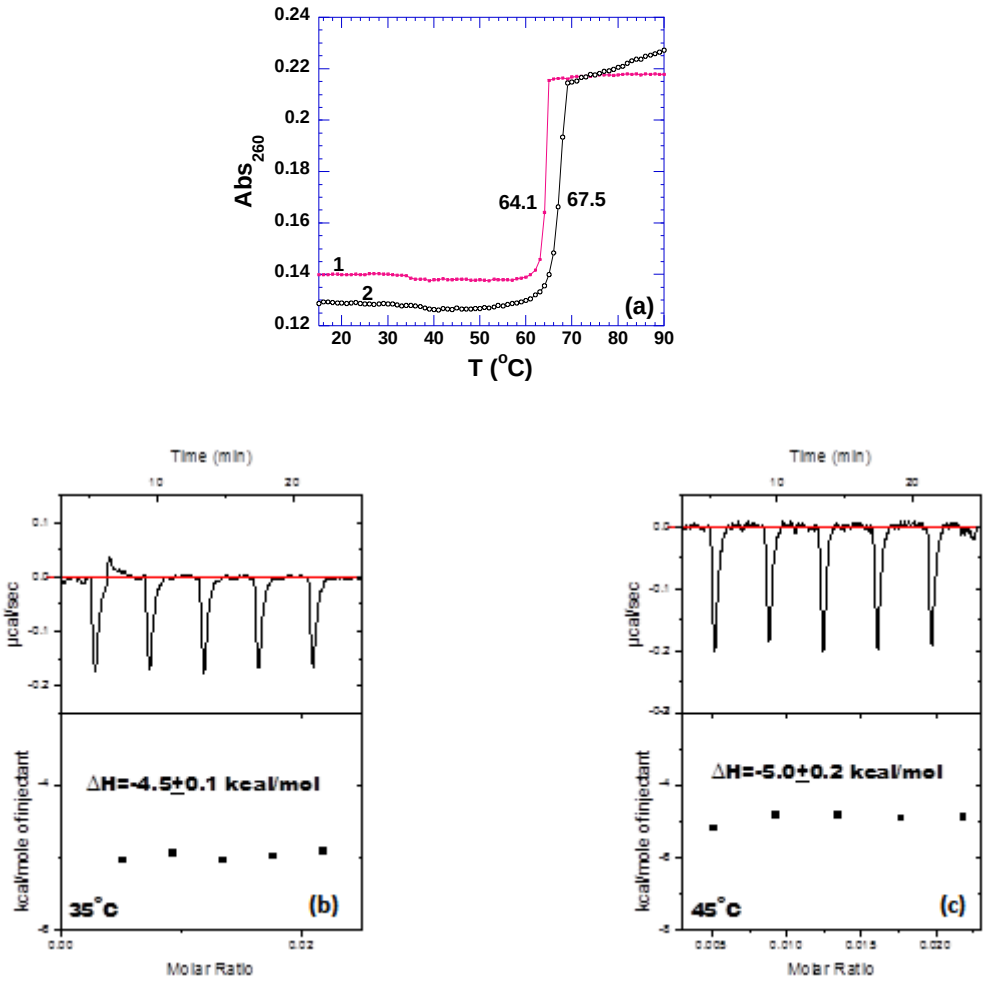

Figure S19. (a) UV melting profiles of poly(rA)•poly(dT) duplex in the absence (1) and presence (2) of neomycin at r_{bd} 8. (b,c) ITC titration of neomycin into DNA (100 μM/ base pair) at (b) 35 ^{o}C and (c) 45 ^{o}C. All experiments were carried out in buffer 10 mM sodium cacodylate, 0.5 mM EDTA, 100 mM NaCl at pH 5.5.

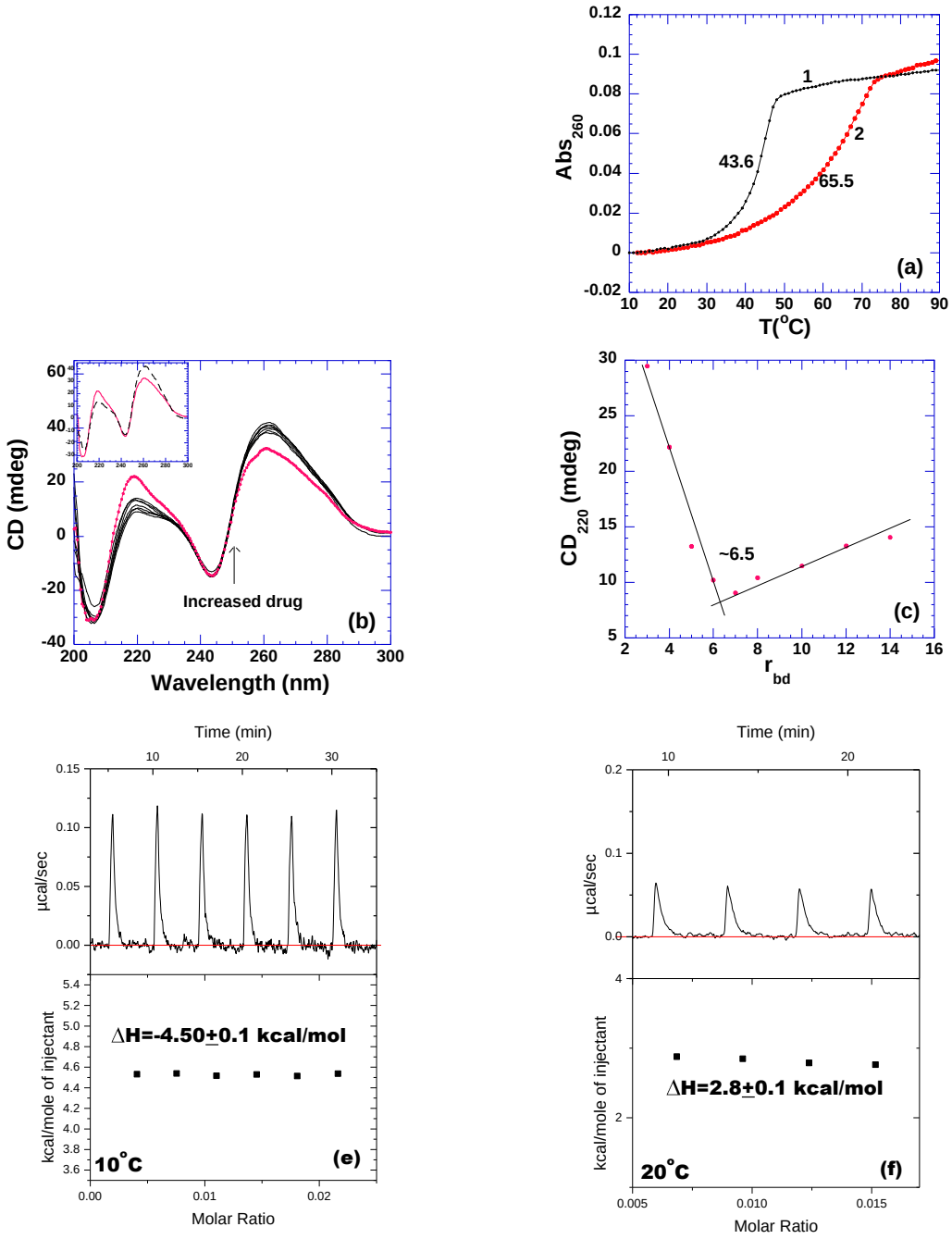

Figure S20. (a) UV melting profiles of poly(dA)•poly(rU) duplex in the absence (1) and presence (2) of neomycin at r_{bd} 6.5. (b) CD scans of neomycin titration with poly(dA)•poly(rU) (75 µM/base pair). The scan with solid circle represents hybrid alone. The inset shows CD spectra of hybrid alone (continuous line) and ligand-saturated complex (dashed line). (c) A plot of CD signals at 243 nm versus corresponding r_{bd}

values. The cross of two apparent linear portions reveals binding site sites. (d,e) ITC titration of neomycin into target (200 μM/base pair) at (d) 10 ^{o}C and (e) and 20 ^{o}C. All experiments were carried out in buffer 10 mM sodium cacodylate, 0.5 mM EDTA, 100 mM NaCl at pH 5.5.

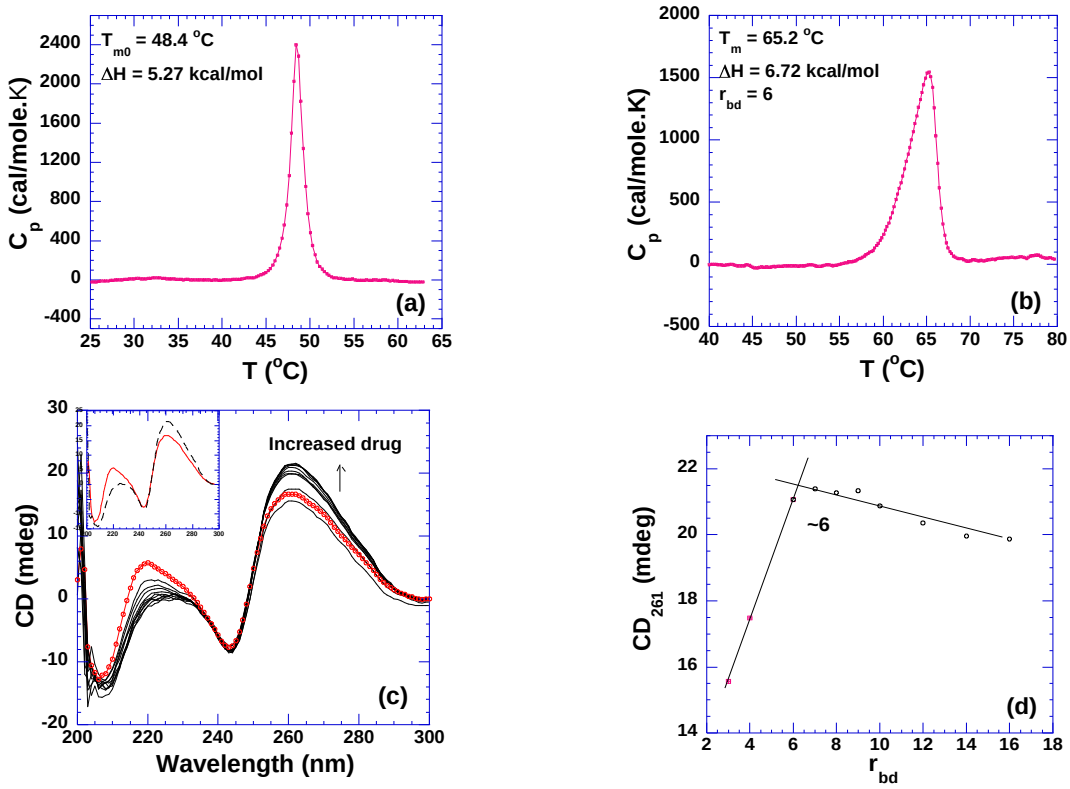

Figure S21. (a,b) DSC melting profiles of poly(dA)•poly(rU) (40 μM/base pair) in the absence (a) and presence (b) of neomycin. (c) CD scans of neomycin titration with poly(dA)•poly(rU) (40 μM/base pair). The scan with solid circle represents DNA alone. The inset shows the CD spectra of DNA alone (continuous line) and ligand-saturated complex (dashed line). (d) A plot of CD signals at 261 nm *vs.* corresponding r_{bd} values. All experiments were carried out in buffer 10 mM sodium cacodylate, 0.5 mM EDTA, 100 mM NaCl at pH 6.8.

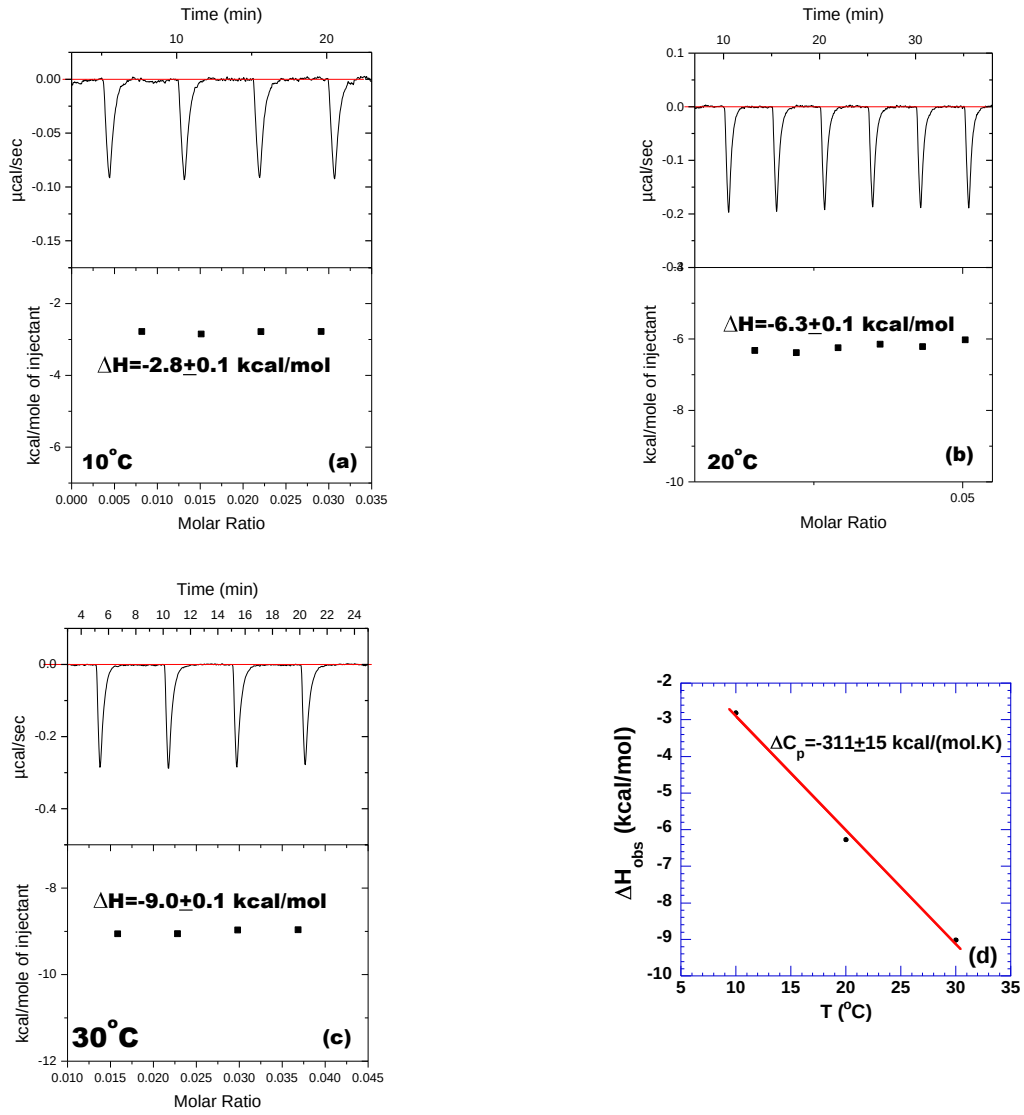

Figure S22. ITC titration of neomycin into poly(dA)•poly(rU) (40 µM/base pair) at (a)10 ^{o}C (b) 20 ^{o}C (c) and 30 ^{o}C (d) A plot of observed binding enthalpy vs. temperature. Slope reveals the heat capacity changes. All experiments were carried out in buffer 10 mM sodium cacodylate, 0.5 mM EDTA, 100 mM NaCl at pH 6.8.

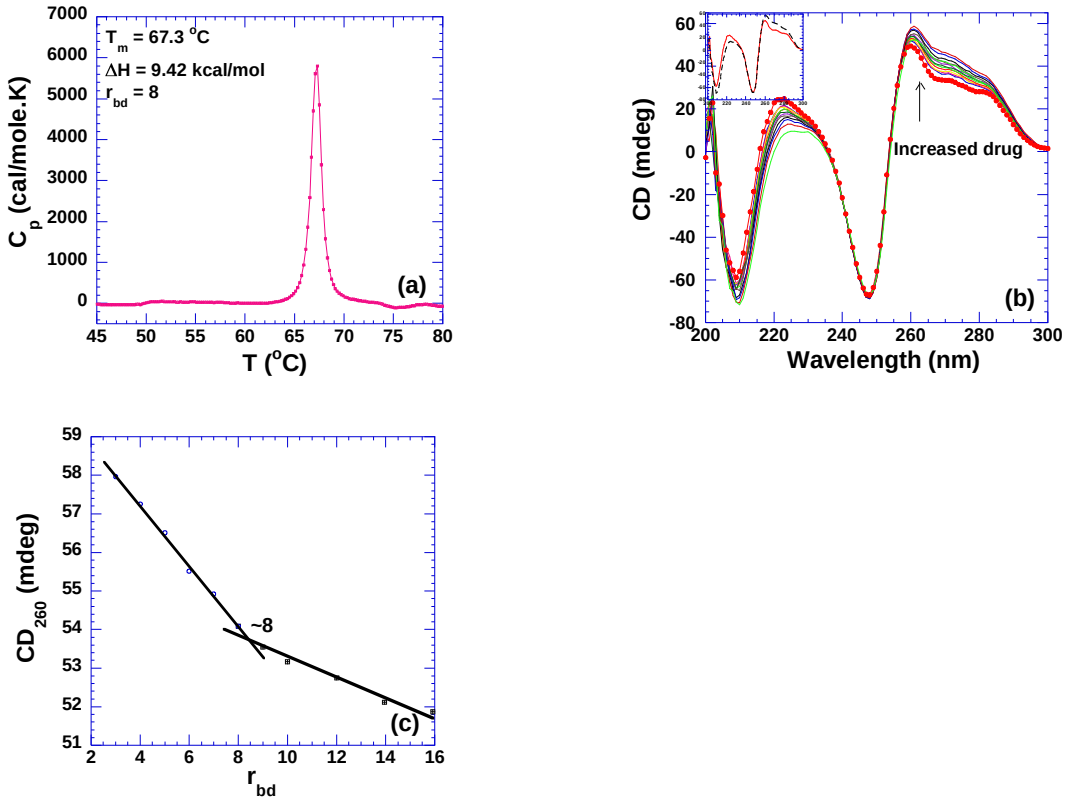

Figure S23. (a) DSC melting profiles of poly(rA)•poly(dT) (100 μM/base pair) in the presence of neomycin at r_{bd} 8. (b) CD scans of neomycin titration with hybrid duplex. CD scans of neomycin titration with poly(rA)•poly(dT) (100 μM/base pair). The scan with solid circle represents hybrid alone. The inset shows CD spectra of hybrid alone (continuous line) and ligand-saturated complex (dashed line). (c) A plot of CD signals at 260 nm vs. corresponding r_{bd} values. All experiments were carried out in buffer 10 mM sodium cacodylate, 0.5 mM EDTA, 100 mM NaCl at pH 6.8.

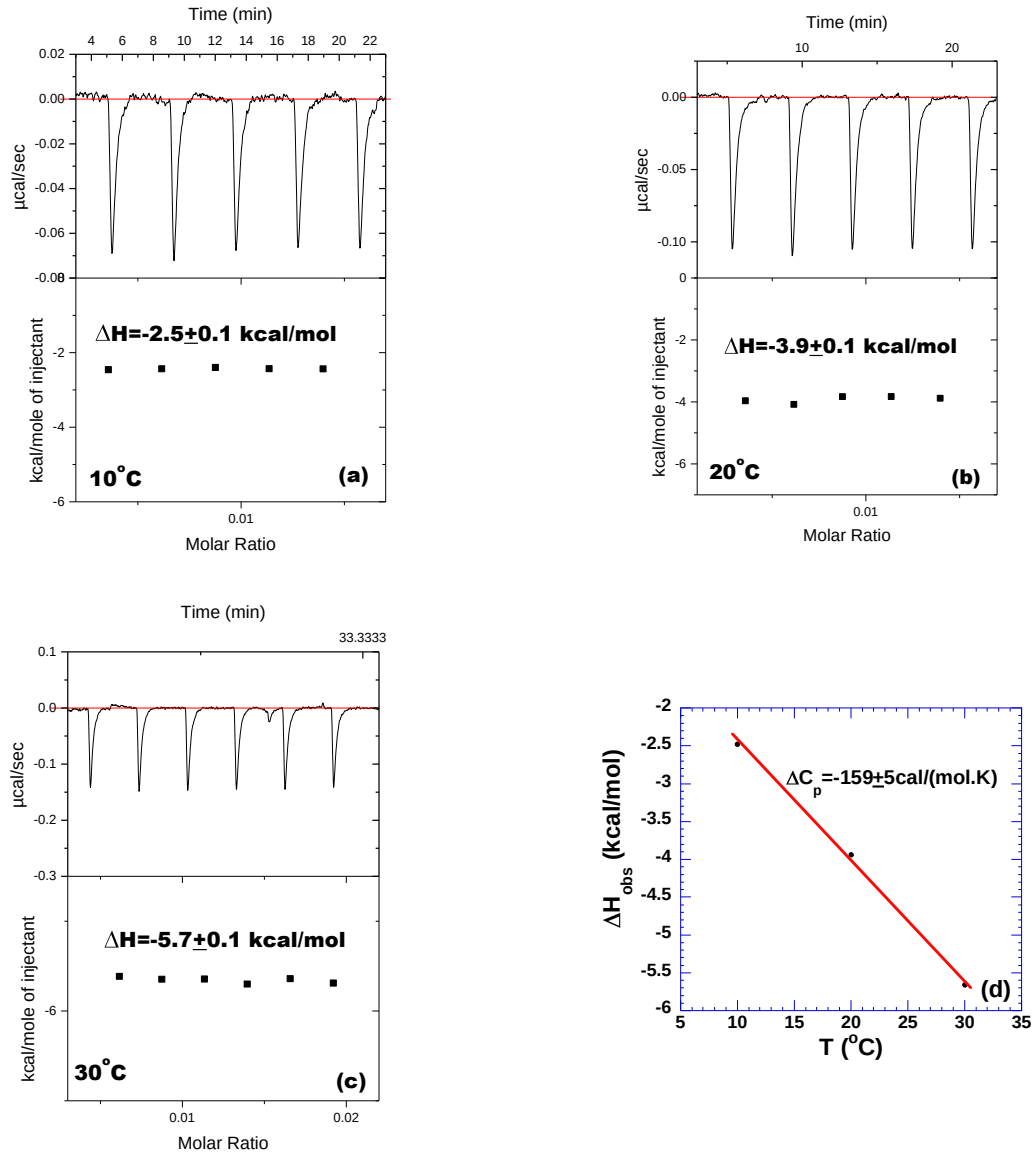

Figure S24. ITC titration of neomycin into poly(rA)•poly(dT) (150 µM/base pair) at (a) 10 ^{o}C (b) 20 ^{o}C (c) and 30 ^{o}C. (d) A plot of observed binding enthalpy *versus* temperature. Slope reveals the heat capacity changes. All experiments were carried out in buffer 10 mM sodium cacodylate, 0.5 mM EDTA, 100 mM NaCl at pH 6.8.

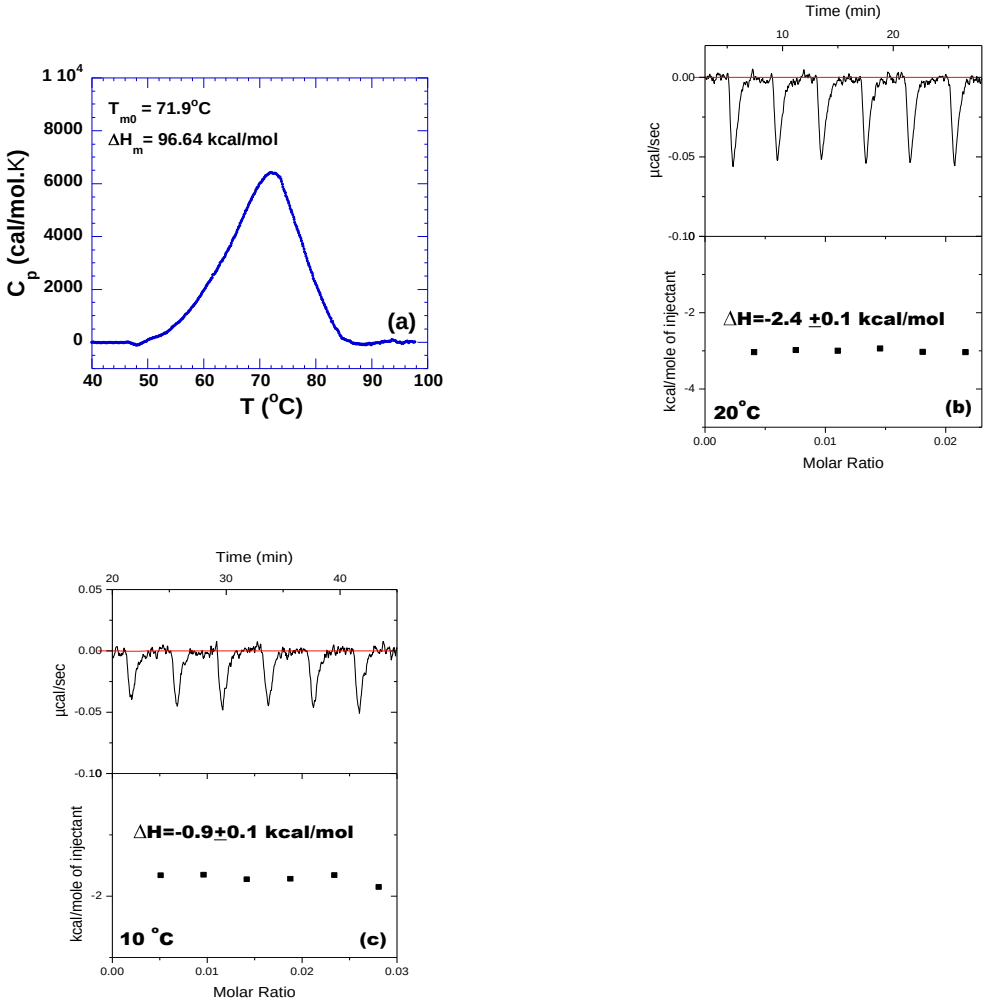

Figure S25. (a) DSC melting profiles of 16S A site rRNA (40 µM/strand) in the absence of neomycin. (b,c) ITC titration of neomycin into A site rRNA (10 µM/strand) at (b) 20 ^{o}C and (c) 10 ^{o}C. All experiments were carried out in buffer 10 mM sodium cacodylate, 0.5 mM EDTA, 100 mM NaCl at pH 5.5.

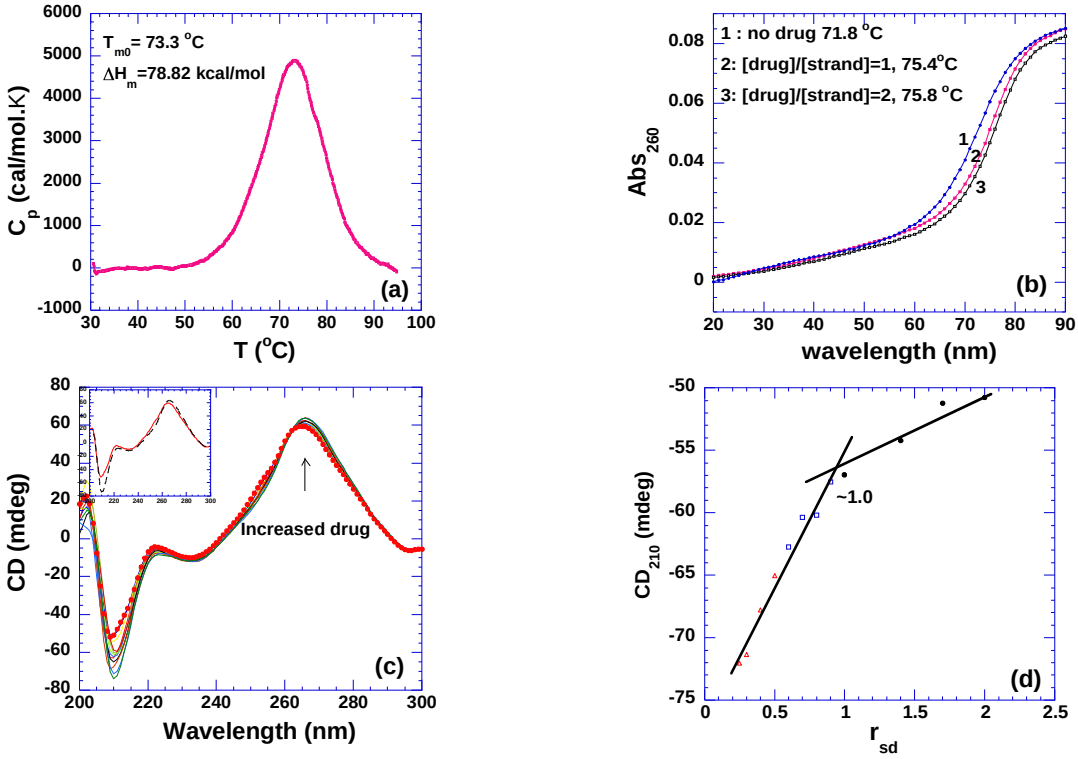

Figure S26. (a) DSC melting profiles of 16S A site rRNA (40 μM/strand) in the absence of neomycin. (b) Thermal stability of A-site rRNA induced by neomycin at r_{dd} 1 and 2. (c) CD scans of neomycin titration with A site rRNA (10 μM/strand). The scan with solid circle represents RNA alone. The inset shows the CD spectra of RNA alone (continuous line) and drug-saturated complex (dashed line). (d) A plot of CD signals at 210 nm *versus* corresponding r_{bd} values. The cross of two apparent linear portions reveals binding site sites. All experiments were carried out in buffer 10 mM sodium cacodylate, 0.5 mM EDTA, 100 mM NaCl at pH 6.8.

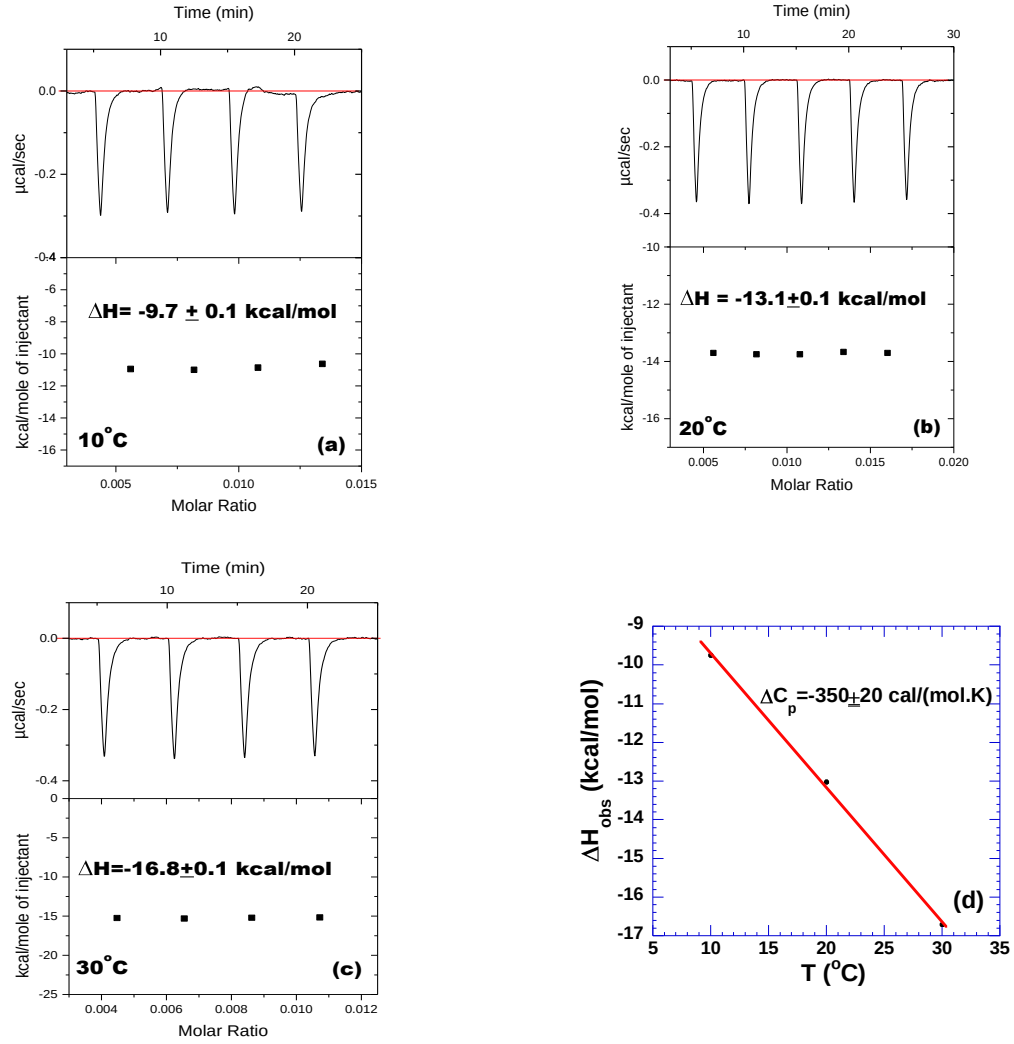

Figure S27. ITC titration of neomycin into 16S A site rRNA (10 µM/strand) at (a) 10 ^{o}C (b) 20 ^{o}C (c) and 30 ^{o}C. (d) A plot of ITC derived ΔH *versus* temperatures. All experiments were carried in out buffer 10 mM sodium cacodylate, 0.5 mM EDTA, 100 mM NaCl at pH 6.8.

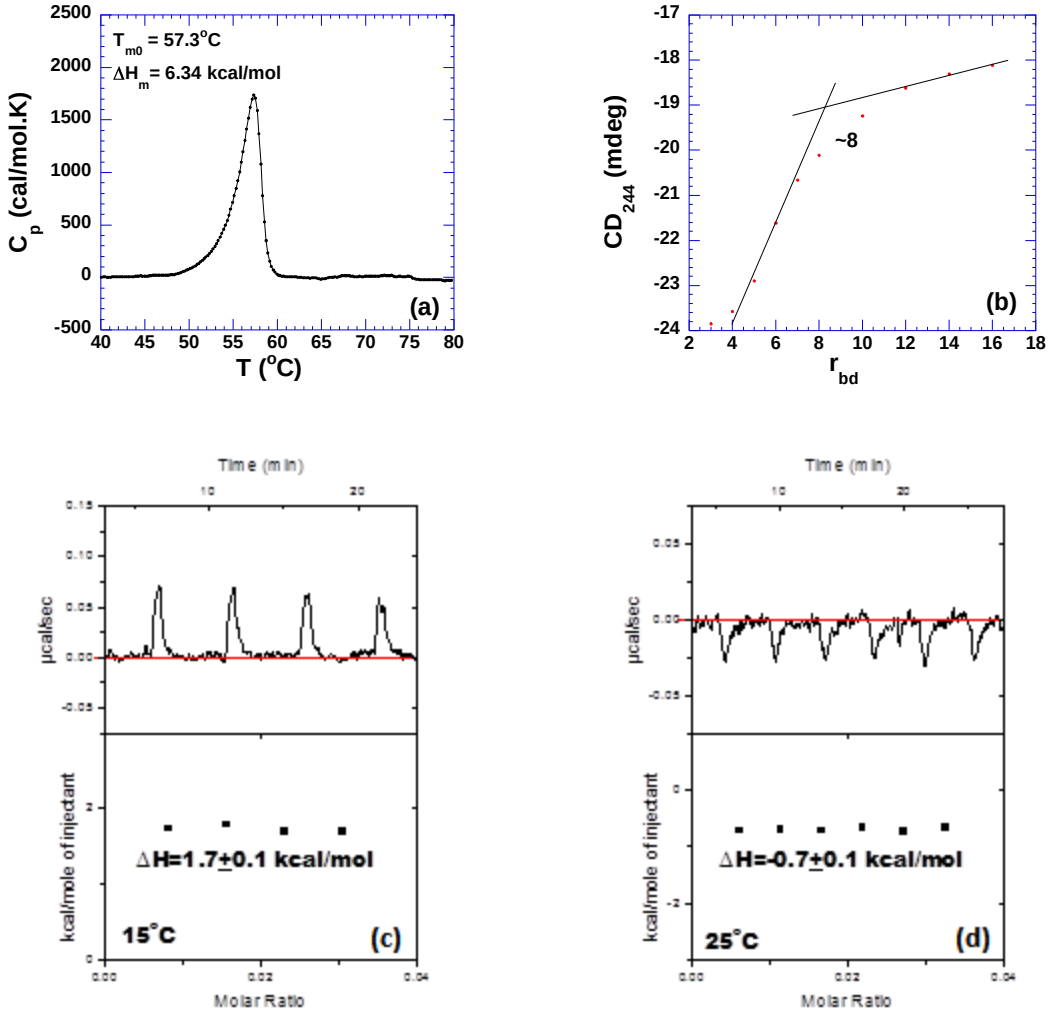

Figure S28. (a) DSC melting profiles of poly(rA)•poly(rU) (150 μM/base pair) in the absence of neomycin. (b) CD scans of neomycin titration with poly(rA)•poly(rU) r_{bd} 8 (16 μM/base pair) . The inset shows the CD spectra of RNA alone (continuous line) and drug-saturated complex (dashed line). (c,d) ITC titration of neomycin into poly(rA)•poly(rU) (200 μM/base pair) at (c) 15 °C and (d) 20 °C. All experiments were carried out in buffer 10 mM sodium cacodylate, 0.5 mM EDTA, 100 mM NaCl at pH 5.5.

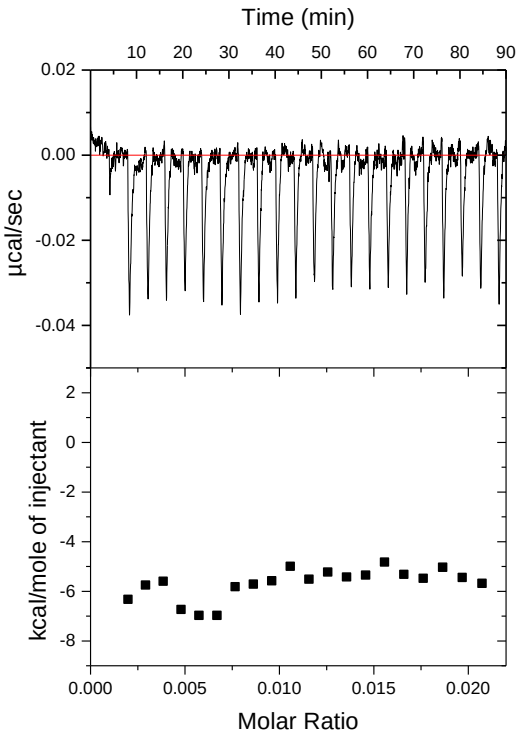

Figure S29. ITC excess site titration heat bursts for neomycin into poly(rA).poly(rU) (150 µM/duplex). Experiment was carried out in buffer 10 mM sodium cacodylate, 0.5 mM EDTA, 100 mM NaCl at pH 6.8, 30 ^{o}C.

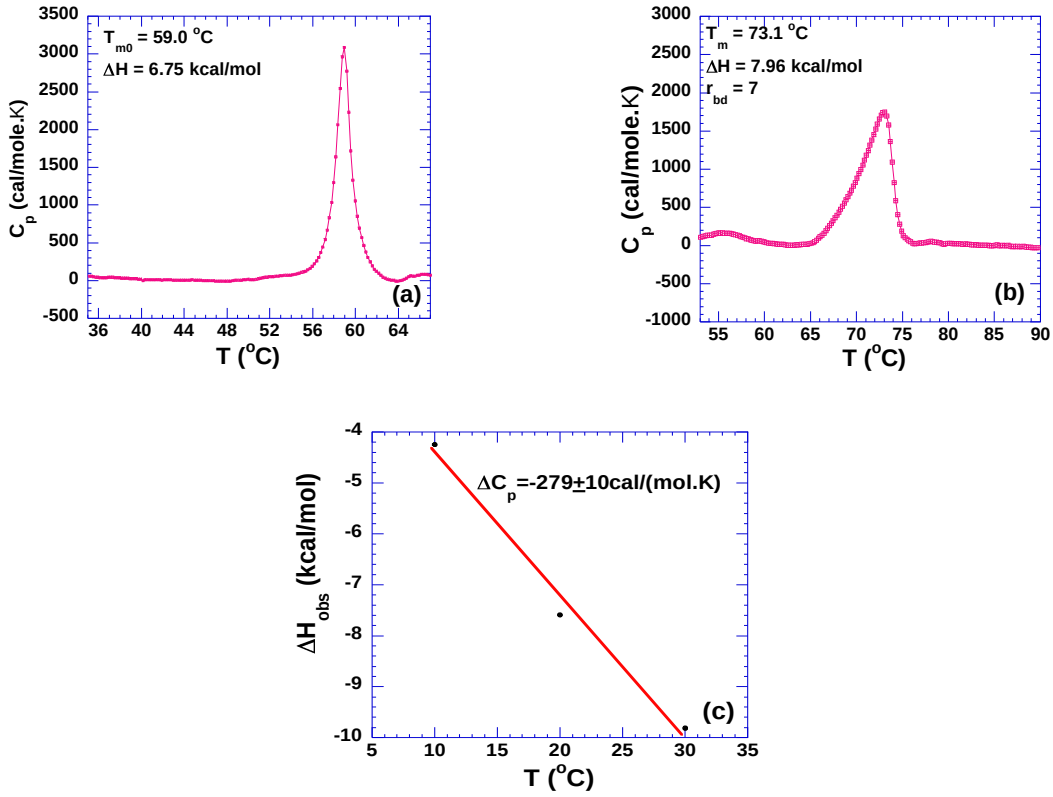

Figure S30. (a,b) DSC melting profiles of poly(rA)•poly(rU) (100 μM/base pair) in (a) the absence and (b) presence of neomycin. (c) A plot of ITC derived ΔH *versus* temperatures. The slope is the heat capacity changes. All experiments were carried out in buffer 10 mM sodium cacodylate, 0.5 mM EDTA, 100 mM NaCl at pH 6.8.

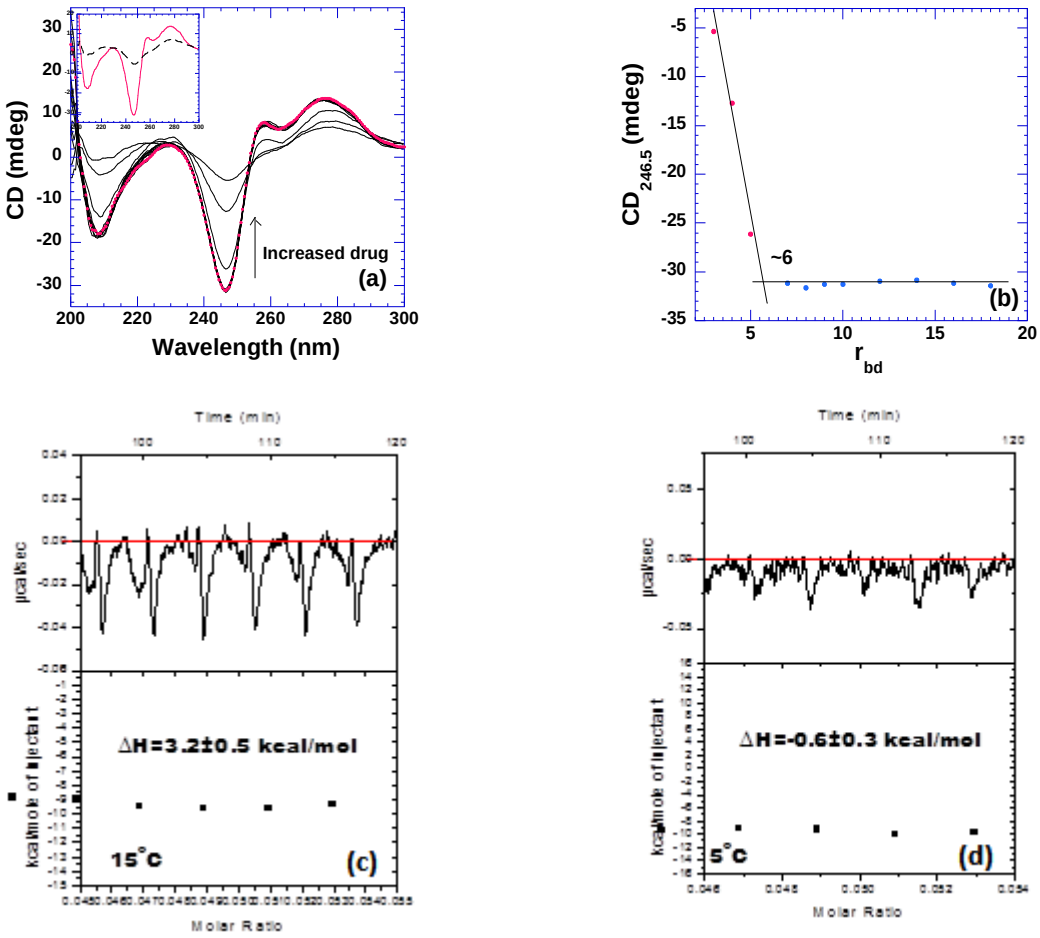

Figure S31. (a) CD scans of neomycin titration with poly(dA)•2poly(dT) (75 µM/base triplet). The inset shows the CD spectra of RNA alone (continuous line) and drug-saturated complex (dashed line). (b) A plot of CD signals at 246 nm *versus* corresponding r_{bd} values. The cross of two apparent linear portions reveals binding site size. (c,d) ITC titration of neomycin into poly(dA)•2poly(dT) (100 µM/base triplet) at (c) 15 ^{o}C and (d) 5 ^{o}C. All experiments were carried out in buffer 10 mM sodium cacodylate, 0.5 mM EDTA, 100 mM NaCl at pH 5.5.

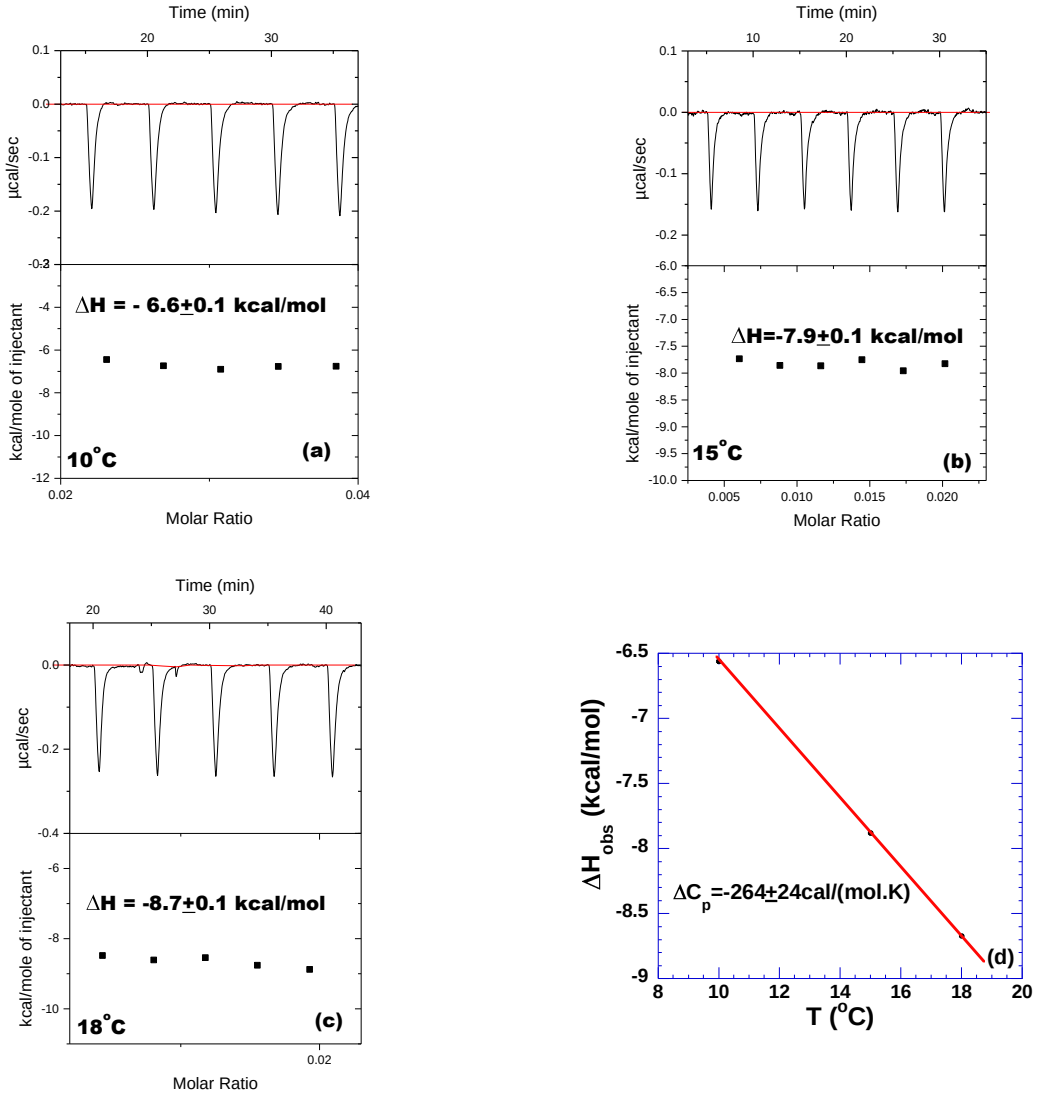

Figure S32. ITC titration of neomycin into poly(dA)•2poly(dT) (150 µM/base triplet) at (a) 10 ^{o}C, (b) 15 ^{o}C, and (c) 18 ^{o}C. (d) A plot of ITC derived ΔH *versus* temperatures. All experiments were carried out in buffer 10 mM sodium cacodylate, 0.5 mM EDTA, 100 mM NaCl at pH 6.8.

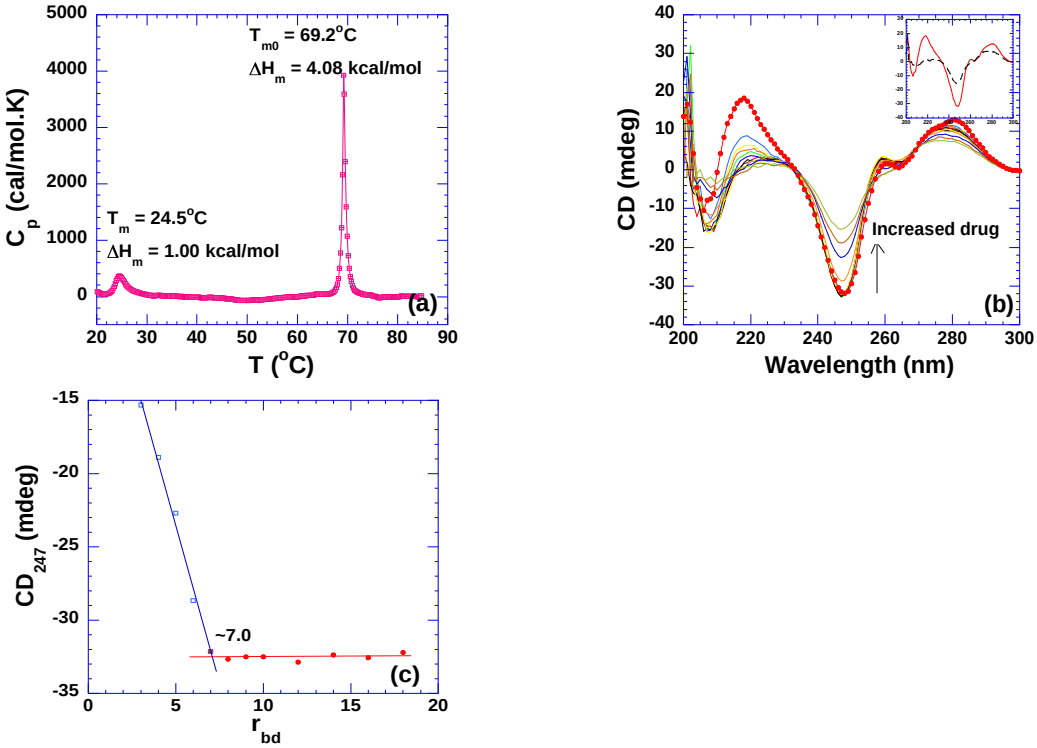

Figure S33. (a) DSC melting profiles of poly(dA)•2poly(dT) (100 μM/base triplet) in the absence of neomycin. (b) CD scans of neomycin titration with poly(dA)•2poly(dT) (75 μM/base triplet). The scan with solid circle represents DNA alone. The inset shows the CD spectra of RNA alone (continuous line) and drug-saturated complex (dashed line). (c) A plot of CD signals at 247 nm *vs.* corresponding r_{bd} values. The cross of two apparent linear portions reveals binding site sizes. All experiments were carried out in buffer 10 mM sodium cacodylate, 0.5 mM EDTA, 100 mM NaCl at pH 6.8.

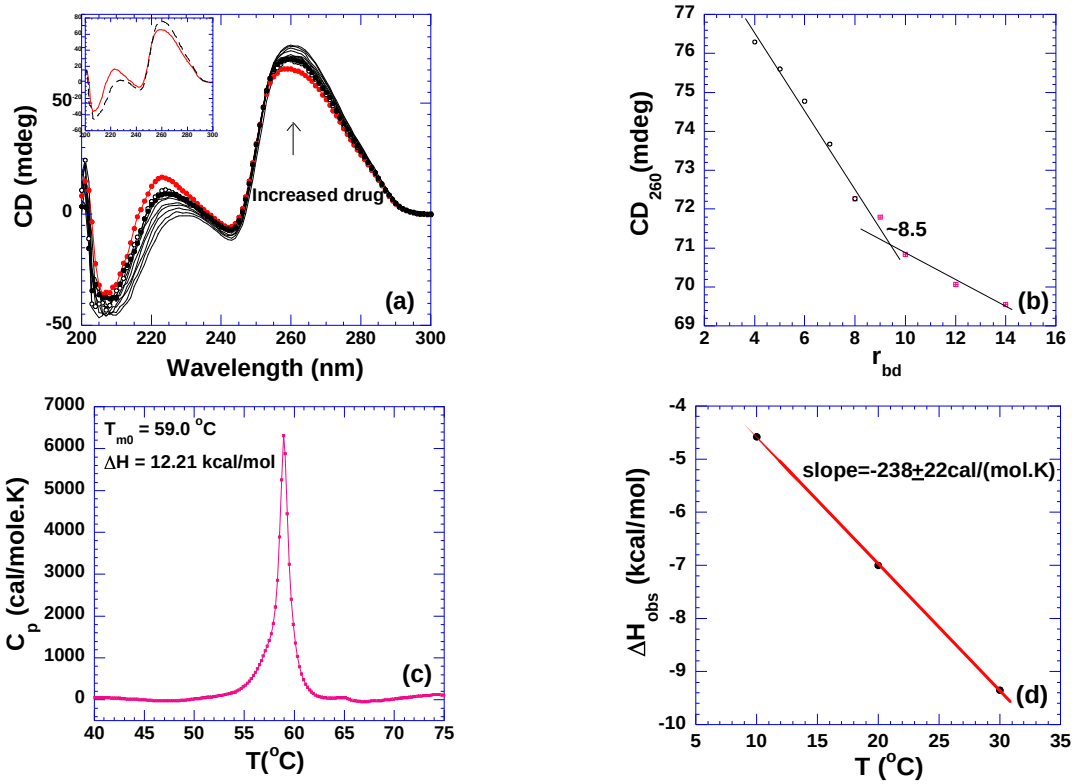

Figure S34. (a) CD scans of neomycin titration with poly(rA)•2poly(rU) (75 μM/base triplet). The scan with solid circle is the one of RNA alone. The inset shows the CD spectra of RNA alone (continuous line) and drug-saturated complex (dashed line). (b) A plot of CD signals at 260 nm *vesus* corresponding r_{bd} values. The cross of two apparent linear portions reveals binding site sites. (c) DSC melting profile of poly(rA)•2poly(rU) (100 μM/base triplet) in the absence of neomycin at r_{bd} 8.5. (d) A plot of ITC derived ΔH_{obs} *versus* temperatures. All experiments were carried out in buffer 10 mM sodium cacodylate, 0.5 mM EDTA, 100 mM NaCl at pH 6.8.

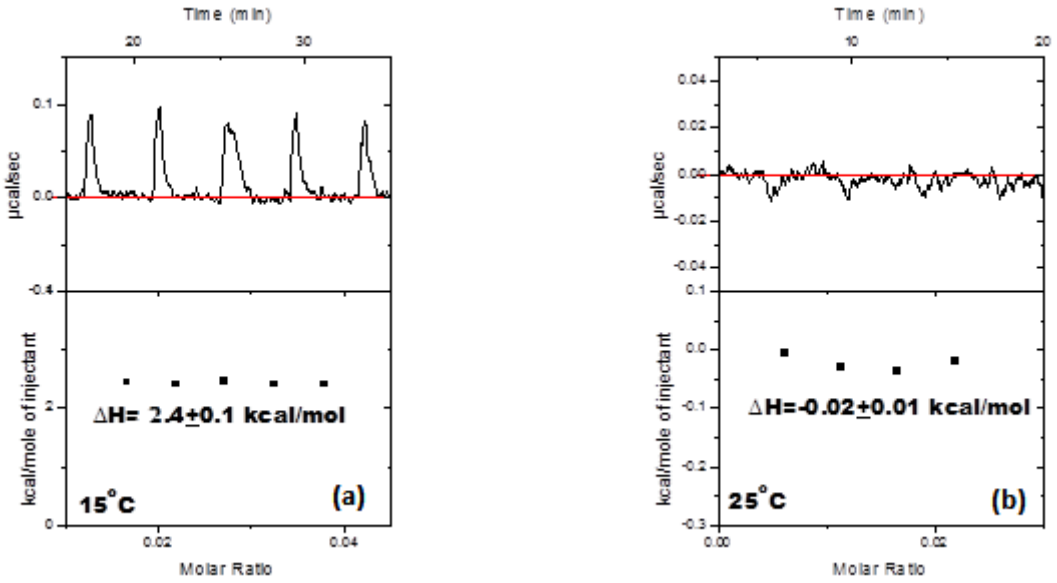

Figure S35. (a,b) ITC titration of neomycin into poly(rA)•2poly(rU) (200 µM/base triplet) at (a) 15 ^{o}C and (b) 25 ^{o}C. All experiments were carried out in buffer 10 mM sodium cacodylate, 0.5 mM EDTA, 100 mM NaCl at pH 5.5.

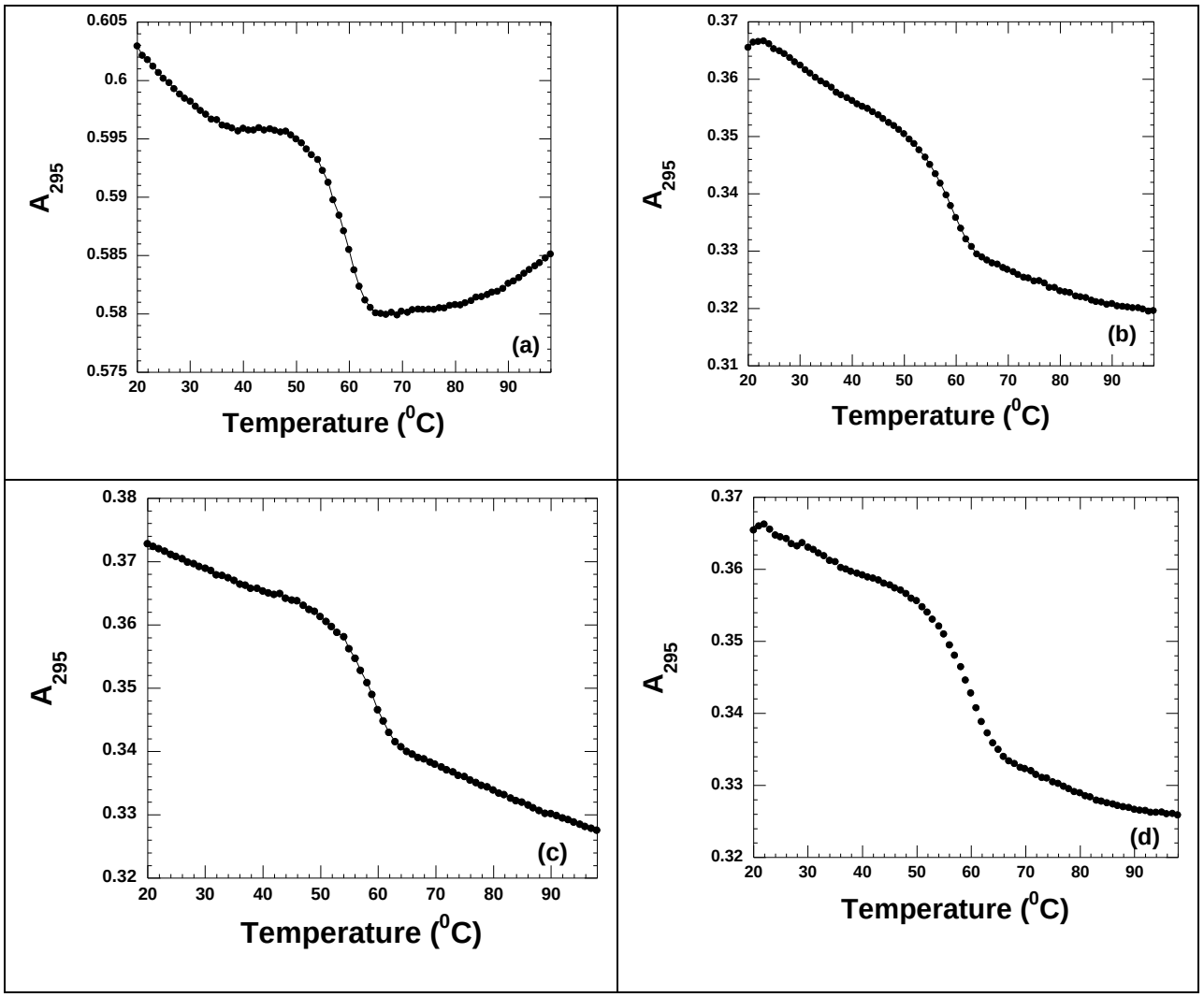

Figure S36. UV thermal denaturation profiles of *Oxytricha* telomeric quadruplex in the absence or presence of neomycin (at 1:1 ratio) at different pH (a) in the absence of neomycin at pH 5.5 (b) in the presence of neomycin at pH 5.5 (c) in the absence of neomycin at pH 6.8 (d) in the presence of neomycin at pH 6.8. All experiments were performed in buffer 10 mM sodium cacodylate, 0.5 mM EDTA, 100 mM NaCl. The concentration of DNA was 2 μM/strand.

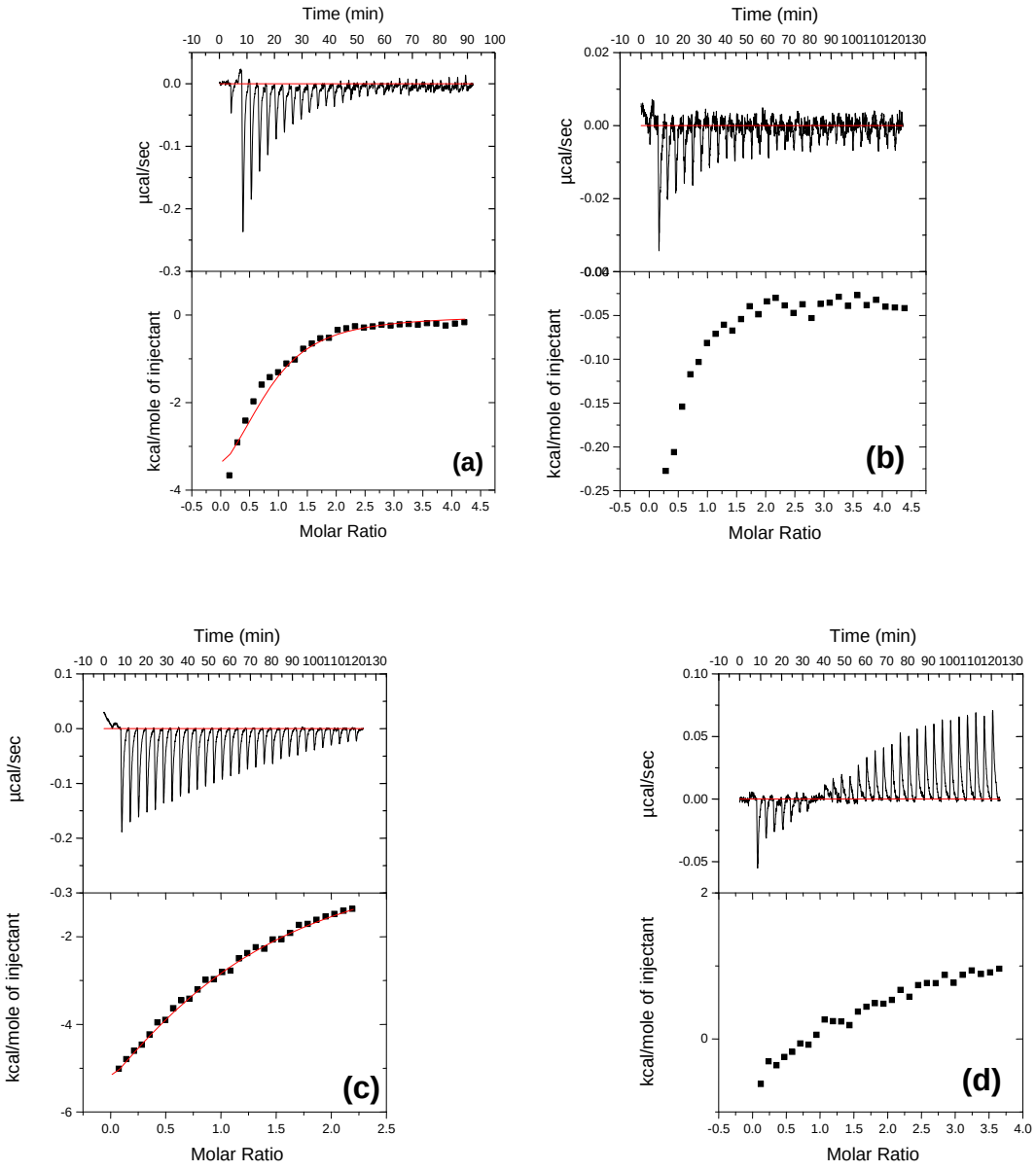

Figure S37. ITC titration of neomycin into (a,b) *Oxytricha nova* telomeric DNA (60 uM/strand) and (c,d) human telomeric DNA (60 uM/strand) at pH's 5.5 and 6.8 respectively. The heat burst curves have been corrected for diltion. All experiments were carried out in buffer 10 mM sodium cacodylate, 0.5 mM EDTA, 100 mM NaCl.

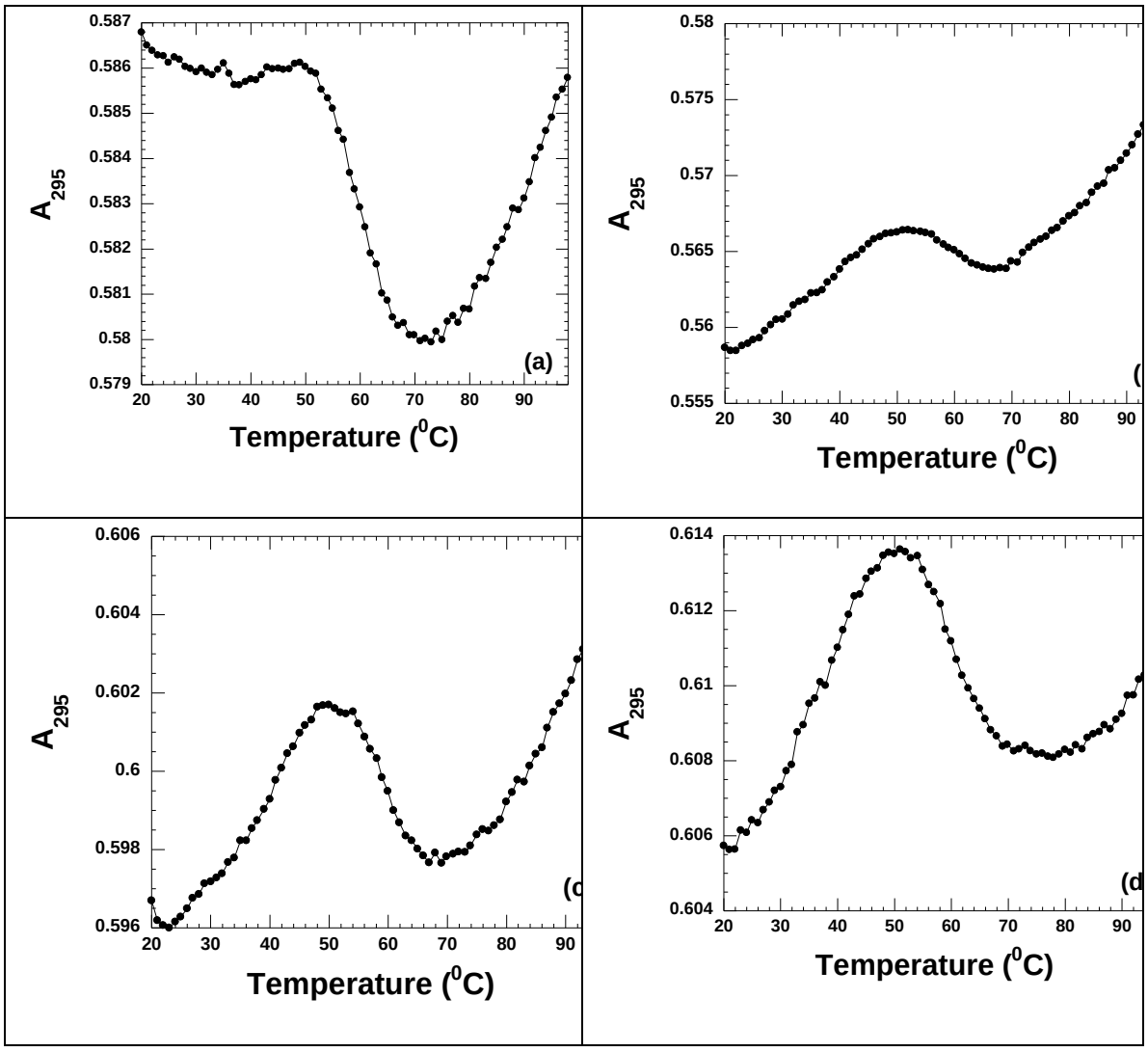

Figure S38. UV thermal denaturation profiles of human telomeric quadruplex in the absence or presence of neomycin (at 1:1 ratio) at different pH (a) in the absence of neomycin at pH 5.5 (b) in the presence of neomycin at pH 5.5 (c) in the absence of neomycin at pH 6.8 (d) in the presence of neomycin at pH 6.8. All experiments were performed in buffer 10 mM sodium cacodylate, 0.5 mM EDTA, 100 mM NaCl. The concentration of DNA was 2 μM/strand.

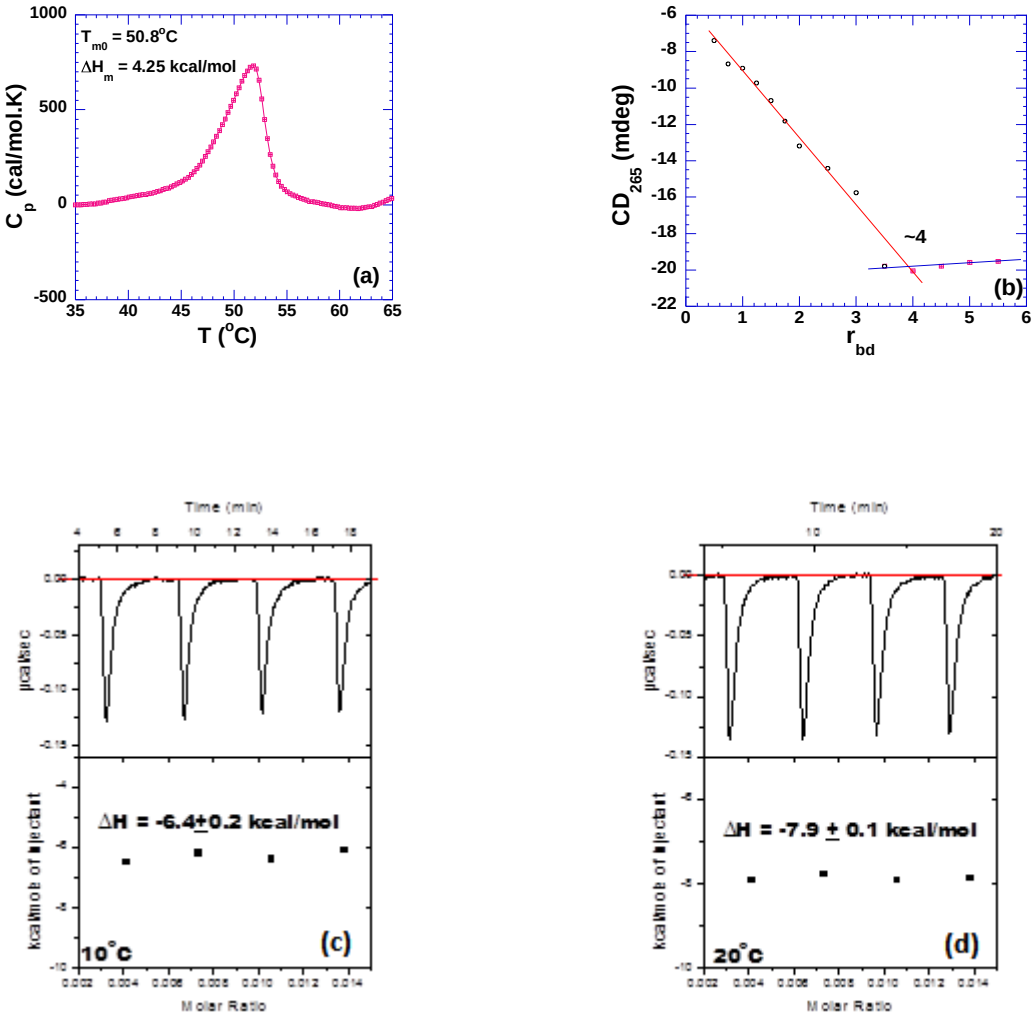

Figure S39. (a) DSC melting profiles of i-motif DNA in the absence of neomycin (150 µM/tetrad). (c) A plot of CD signals at 266 nm *versus* corresponding r_{bd} values. The cross of two apparent linear portions reveals binding site sites. (c,d) ITC titration of neomycin into DNA at (120 µM/tetrad) (c) 10 ^{o}C and (d) 20 ^{o}C. All experiments were carried out in buffer 10 mM sodium cacodylate, 0.5 mM EDTA, 100 mM NaCl at pH 6.8.

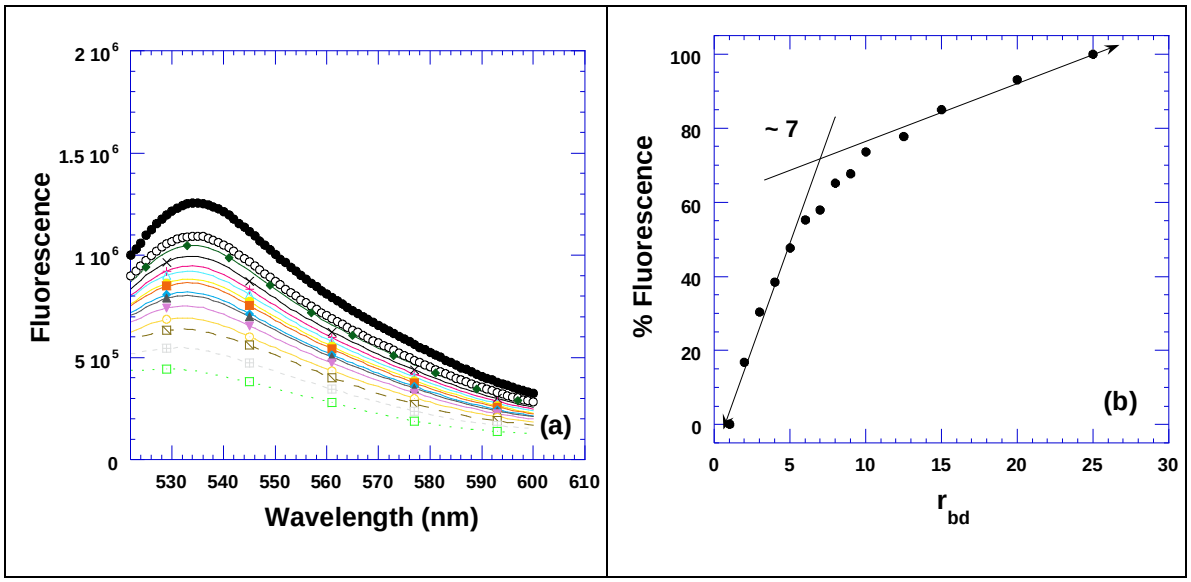

Figure S40. (a) Fluorescence titration of neomycin into poly(rA).poly(dT) (15 μM/base pair). (b) A plot of fluorescence intensity *versus* corresponding r_{bd} values. The cross of two apparent linear portions reveals r_{bd} ~7. Experiment was carried out in buffer 10 mM sodium cacodylate, 0.5 mM EDTA, 100 mM NaCl at pH 6.8.

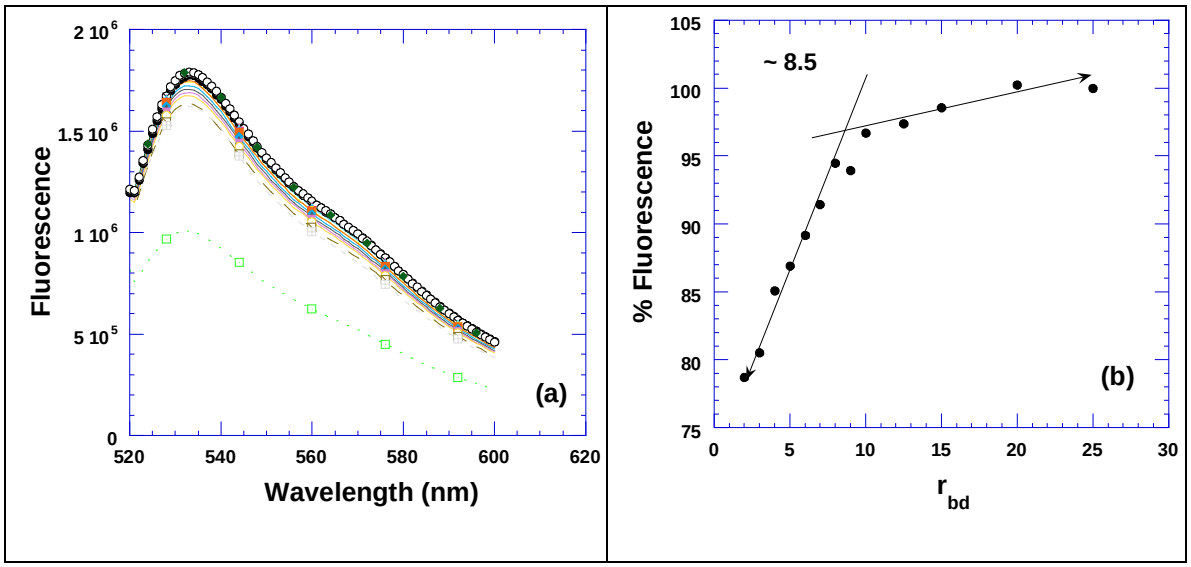

Figure S41. (a) Fluorescence titration of neomycin into poly(dA-dT)$_2$ (15 μM/base pair). (b) A plot of fluorescence intensity *versus* corresponding r_{bd} values. The cross of two apparent linear portions reveals r_{bd} ~8.5. Experiment was carried out in buffer 10 mM sodium cacodylate, 0.5 mM EDTA, 100 mM NaCl at pH 6.8.

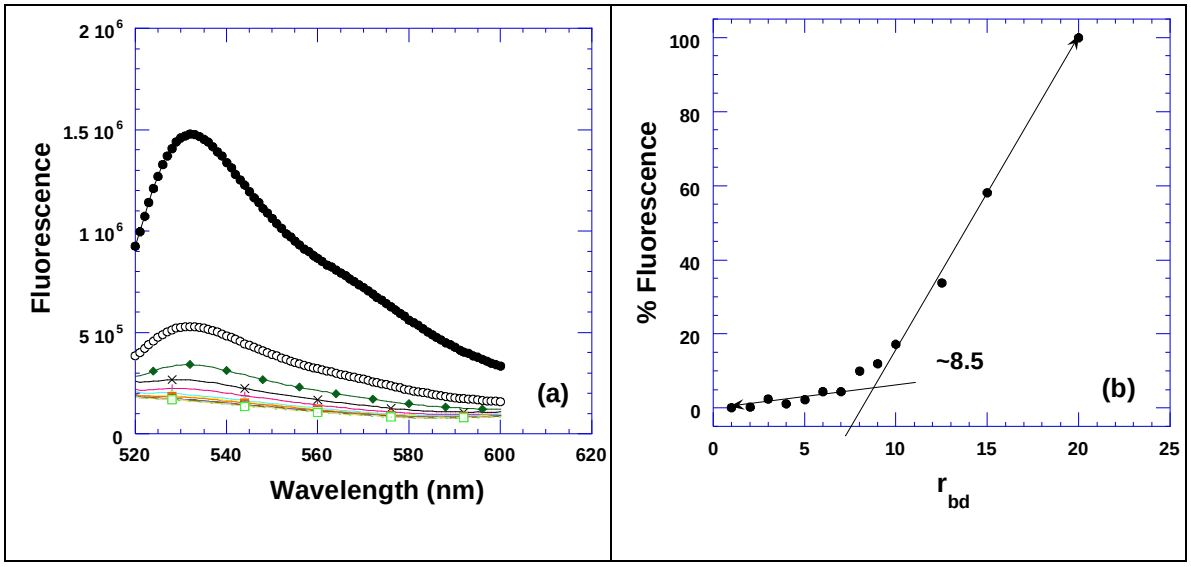

Figure S42. (a) Fluorescence titration of neomycin into poly(rA).poly(rU) (15 μM/base pair). (b) A plot of fluorescence intensity *versus* corresponding r_{bd} values. The cross of two apparent linear portions reveals r_{bd} ~8.5. Experiment was carried out in buffer 10 mM sodium cacodylate, 0.5 mM EDTA, 100 mM NaCl at pH 6.8.

Table S1. Computer generated models for neomycin bound to various nucleic acids as suggested by docking studies using Autodock Vina 1.0.

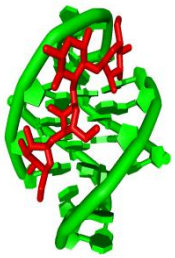	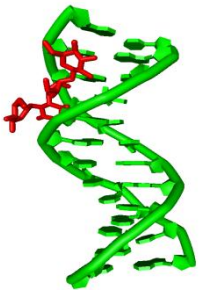		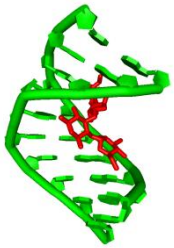	
156D·neomycin	1BNA·neomycin	1D3R·neomycin	440D·neomycin	406D·neomycin
	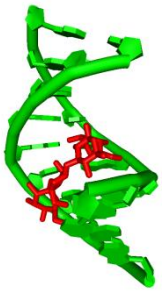	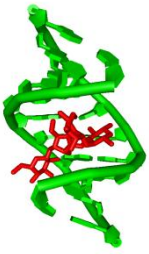	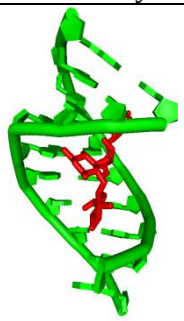	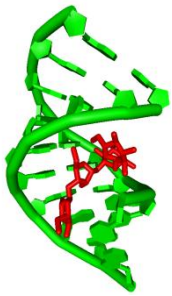
1DC0·neomycin	1ZEX·neomycin	1ZEY·neomycin	1ZF1·neomycin	1ZF6·neomycin
		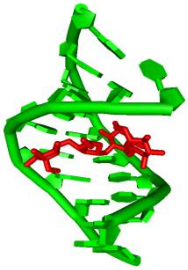		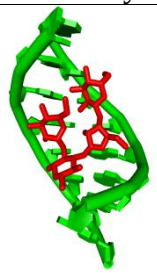
1ZF8·neomycin	1ZF9·neomycin	1ZFA·neomycin	1ZFJ·neomycin	2ANA·neomycin
				
2ETA4·neomycin	3ZNA·neomycin	143D·neomycin		

Table S2. Computer generated data for neomycin bound to various nucleic acids as a as determined according to structure. Results report binding affinity as a function of groove width. PDB identification correlates with models represented in Table S1.

Nucleic Acid	Sequence	PDB ID	Length (mer)	Groove Width (Å)	Binding Affinity (kcal/mol)
A-Form Duplex	d-5'(AGGGGCGGGGCT) d-5'(TAGCCCCGCCCC)	1ZJF	12	9.0	-9.8
RNA A-Form	R(CACCGGAUGGU(5BU)CGGUG)	406D	13	9.3	-10
Synthetic Z Form DNA	d-5'(CGCGCGCGCGCG)	3ZNA	12	13.3	-7.8
Quadplex *Oxytricha Nova*	d-5'(GGGGTTTTGGGG)	156D	12	14.3	-7.2
B-Form Duplex (Major Groove)	d-5'(CGCGAATTCGCG)	1BNA	12	16.5	-7.3
Quadruplex Human	d-5'(AGGGTTAGGGTTAGGGTTAGGG)	143D	22	15.8	-7.1

Table S3. A-form nucleic acid structures bound to neomycin and modeled according to content and length. Results report binding affinity as a function of groove width. PDB identification correlates with models represented in Table S1.

DNA Type	Sequence	PDB ID	Length (mer)	Groove Width (Å)	Binding Affinity (kcal/mol)
A-form DNA	d-5'(AGGGGCGGGGCT) d-5'(TAGCCCCGCCCC)	1ZJF	12	8.5	-9.8
A-form DNA	d-5'(CCCCATGGGG)	1ZF6	10	6.9	-9.4
A-form DNA	d-5'(CATGGGCCCATG)	1DC0	12	14.3	-8.8
A-form DNA	d-5'(AGGGGCCCCT)	440D	10	10.0	-8.7
A-form DNA	d-5'(CCCGGCCGGG)	1ZEX	10	8.2	-8.7
A-form DNA	d-5'(CCCCGCGGGG)	1ZEY	10	8.5	-8.7
A-form DNA	d-5'(CCCCCGGGGG)	1ZF9	10	8.8	-8.6
A-form DNA	d-5'(CCGGGCCCGG)	1ZF1	10	9.2	-8.4
A-form DNA	d-5'(CCTCCGGAGG)	1ZFA	10	8.8	-8.3
A-form DNA	d-5'(CCACCGGTGG)	1ZF8	10	10.7	-8.2
A-form DNA	d-5'(GGGGCCCC)	2ANA	8	12.5	-8.1

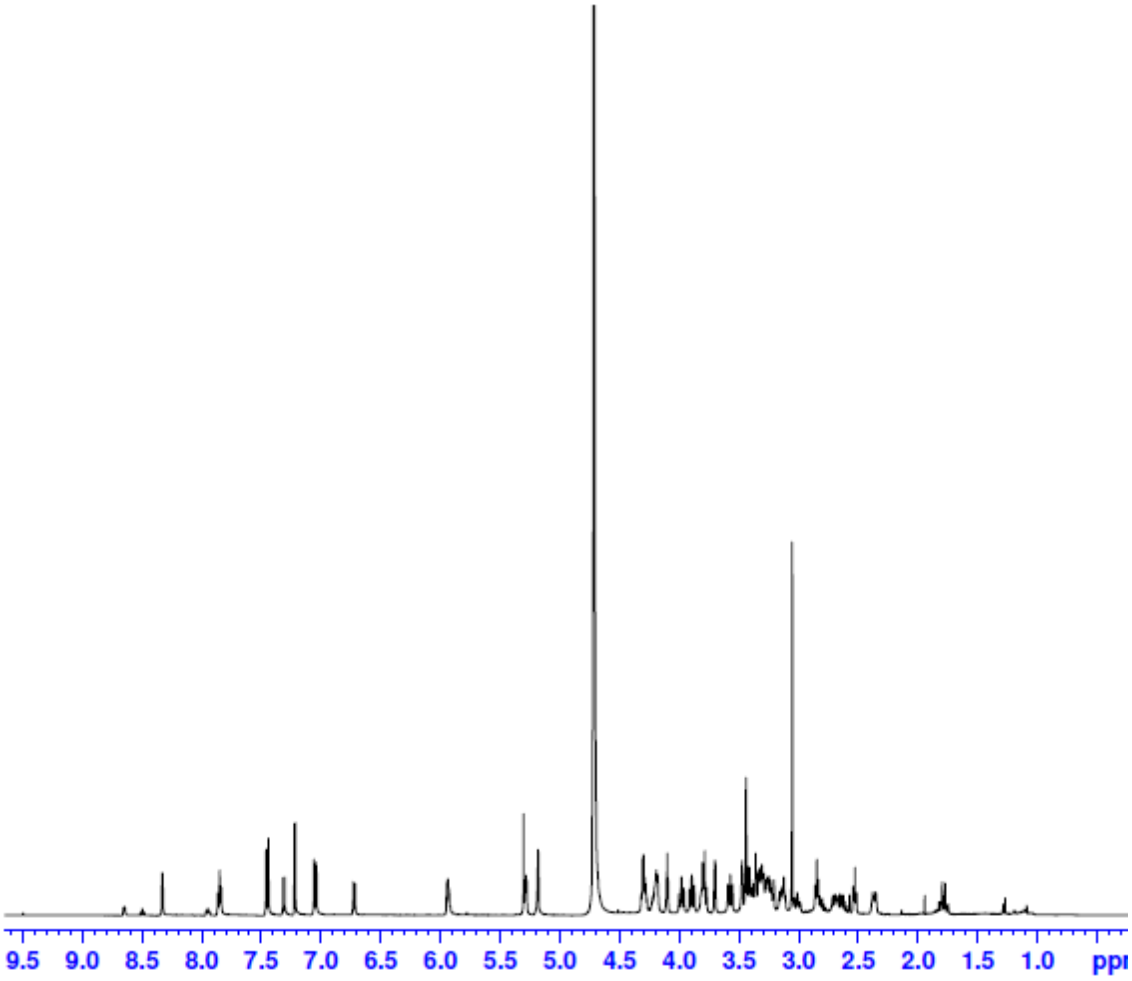

Figure S43. 1H NMR of fluorescein-neomycin (**F-neo**) conjugate **4**.

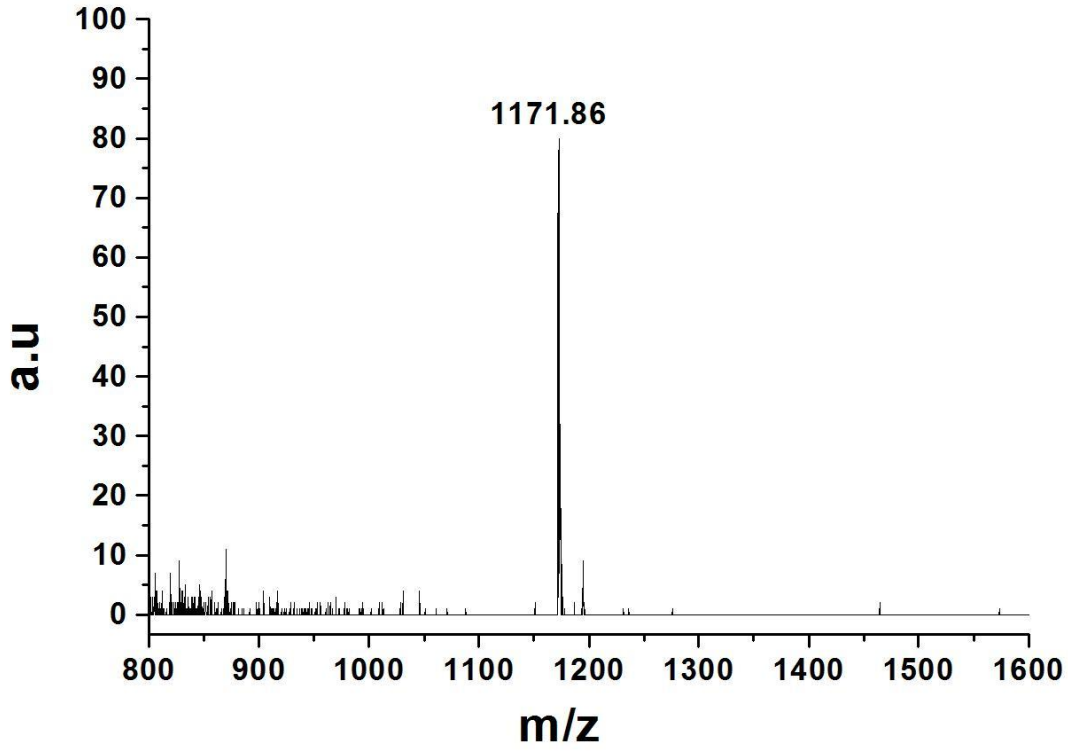

Figure S44. MALDI-TOF spectra of fluorescein-neomycin (**F-neo**) conjugate **4**.